Tectonophysics 723 (2018) 41–55

Contents lists available at ScienceDirect

Tectonophysics

journal homepage: www.elsevier.com/locate/tecto

Paleomagnetism of the Permian-Triassic intrusions from the Tunguska syncline and the Angara-Taseeva depression, Siberian Traps Large Igneous Province: Evidence of contrasting styles of magmatism

Latyshev A.V.[a,b,*], Veselovskiy R.V.[a,b], Ivanov A.V.[c]

[a] Schmidt Institute of the Physics of the Earth, Russian Academy of Sciences, Moscow, Russia
[b] Lomonosov Moscow State University, Geological Department, Russia
[c] Institute of the Earth's Crust, Siberian Branch of the Russian Academy of Sciences, Irkutsk, Russia

ARTICLE INFO

Keywords:
Paleomagnetism
Large Igneous Province
Siberian Traps
Secular variations
Permian
Triassic

ABSTRACT

Based on the detailed paleomagnetic investigation, we distinguished different styles of intrusive magmatic activity in two regions of the Siberian Traps Large Igneous Province (LIP). The emplacement of intrusions in the Angara-Taseeva depression (the southern periphery of the Siberian Traps LIP) occurred as brief but intense bursts of magmatic activity that led to the emplacement of large and extensive sills. We argue that this pulsating style of intrusive magmatic activity is common for the margins of the Siberian Traps LIP. We also estimated the duration of the main magmatic events as $< 10^4$–10^5 years for the large sills and their area of manifestation ($>$ 200–250 km in diameter and dozens of thousands km^2 in square). On the contrary, in the central part of the Siberian Traps LIP (the Tunguska syncline) the intrusive magmatism was more or less continuous without intense peaks of magmatic activity. Furthermore, we obtained the first reliable magnetostratigraphic data from the volcanic section of the Tunguska syncline. Finally, we analyzed the available paleomagnetic and geochronological data from the Siberian platform and suggested the correlation scheme of the studied intrusive complexes with the volcanic sequences of the Siberian Traps LIP.

1. Introduction

The Siberian Traps Large Igneous Province (LIP) is the object of many investigations on its origin and the emplacement duration (e.g. Reichow et al., 2009; Sobolev et al., 2011; Burgess et al., 2017 and many others). The scientific interest to study this enormous area of intraplate magmatic activity resides in a large number of reasons. Firstly, the Siberian Traps LIP is considered to be the classic example of the continental LIP magmatism and represents the type area for testing the formation models for such provinces, including the most common mantle plume and other alternative hypotheses (e.g. Czamanske et al., 1998; Elkins-Tanton, 2005; Ivanov, 2007; Sobolev et al., 2011). Secondly, the idea of possible causal link between the Siberian Trap magmatic activity and the global biotic crisis at the Permian-Triassic boundary has been the topic of extensive discussions (e.g. Courtillot and Renne, 2003; Saunders and Reichow, 2009; Burgess and Bowring, 2015). Finally, the unique Cu-Ni and platinum group elements (PGE) deposits of the Norilsk region are localized in the Siberian Traps intrusions, and the genesis of such deposits is still debated (e.g. Naldrett et al., 1996; Krivolutskaya, 2016). To solve all the above-mentioned problems, the detailed and reliable information about the duration of magmatic activity and its intensity, as well as about the correlation of volcanic sections and intrusive complexes, is vital.

The recent U-Pb and ^{40}Ar/^{39}Ar dating established that the main phase of the greatest LIPs formation takes about 1–2 Myr or even less. Such data were obtained, for example, from Deccan (Renne et al., 2015; Schoene et al., 2015), Karoo-Ferrar (Svensen et al., 2012; Burgess et al., 2015; Ivanov et al., 2017), Central Atlantic (Blackburn et al., 2013) and Siberian Traps (Reichow et al., 2009; Burgess and Bowring, 2015) LIPs. However, some geochronologic data suggest that the total magmatic activity in, at least, some of these LIPs could last up to 10–15 Myr and even more (e.g. Jourdan et al., 2007; Ivanov et al., 2013; Sell et al., 2014). The detailed paleomagnetic investigations have led to the significant progress in understanding the dynamics of the volcanic activity. The systematic paleomagnetic studies of lava sections from the Siberian Traps, Deccan and Karoo provinces demonstrated that the lava pile eruption took place as the sequence of very short and intense bursts of volcanic activity ("volcanic pulses", "single eruptive events") interchanging with more prolonged periods of quiescence (Chenet et al., 2008, 2009; Moulin et al., 2011; Pavlov et al., 2011a, 2015).

* Corresponding author at: Schmidt Institute of the Physics of the Earth, Russian Academy of Sciences, Moscow, Russia.
E-mail address: anton.latyshev@gmail.com (A.V. Latyshev).

https://doi.org/10.1016/j.tecto.2017.11.035
Received 22 October 2016; Received in revised form 5 November 2017; Accepted 27 November 2017
Available online 29 November 2017

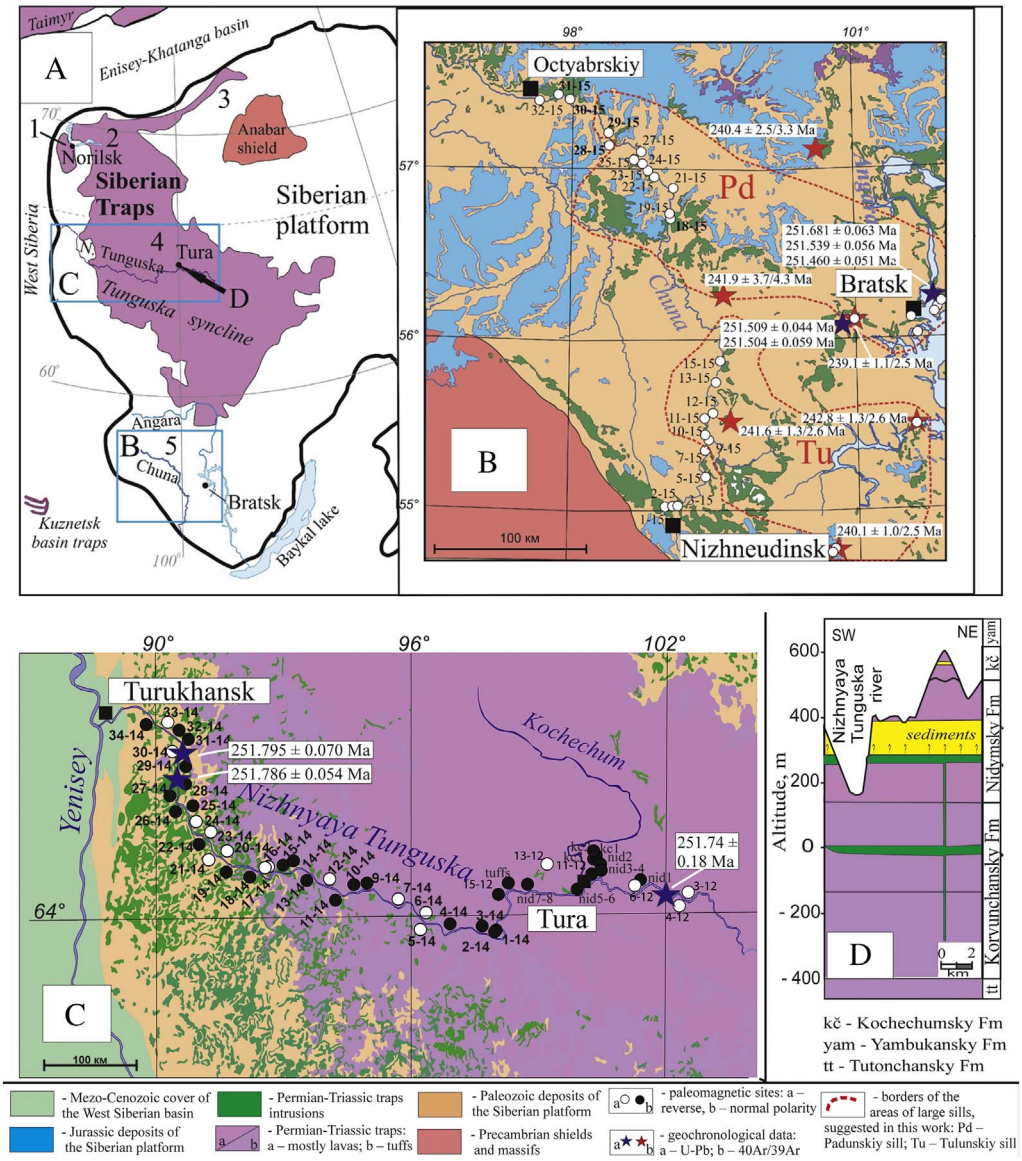

Fig. 1. The sketch geological map of the Siberian Traps province and regions of this study. A – Siberian Traps province and the location of studied areas. The different regions of the LIP within the Siberian platform are shown by numbers: 1 – Norilsk; 2 – Putorana; 3- Maymecha-Kotuy; 4 – Tunguska syncline; 5 – Angara-Taseeva depression. B – Angara-Taseeva depression, the Chuna river valley. Paleomagnetic sites from (Latyshev et al., 2013) used in this work are shown as circles without numbers. C – central part of the Tunguska syncline, the Nizhnyaya Tunguska river valley. D – the sampled part of the volcanic section near Tura (after Ivanov et al., 2013). Geochronological sampling locations: U-Pb – from (Burgess and Bowring, 2015; Paton et al., 2010); 40Ar/39Ar – from (Ivanov et al., 2009, 2013).

As to the Siberian Traps LIP, predominantly "pulsating" style of volcanic activity was shown for the most complete lava sequences of the Norilsk and Maymecha-Kotuy regions in the northern margin of the Siberian platform (Pavlov et al., 2015) (see Fig. 1A for location). Furthermore, intrusive complexes from the southern and eastern periphery of the Tunguska syncline have been used for the detailed paleomagnetic investigations (Latyshev et al., 2013; Konstantinov et al., 2014). For each of the studied regions it was demonstrated that the majority of sampled intrusive bodies were emplaced during several brief and voluminous magmatic events. However, it remains unclear whether the similar style of intrusive magmatic activity is dominant for the inner part of the Siberian Traps LIP or not.

The main goal of this study was to obtain detailed paleomagnetic data from the intrusions of two regions of the Siberian Traps LIP: the Tunguska syncline (the Nizhnyaya (Lower) Tunguska river valley) and the Angara-Taseeva depression (the Chuna river valley) and to compare the timing and dynamics of the magmatic activity in these areas.

2. Geology and sampling sites

The Siberian Traps LIP covers vast areas on the Siberian platform (the Tunguska syncline and surrounding areas) and in the adjacent fold belts. Products of Permian-Triassic magmatic activity are widespread in the Taimyr peninsula (e.g. Gurevitch et al., 1995), West Siberia (Reichow et al., 2005), the Kuznetsk basin (Buslov et al., 2010) (Fig. 1A), as indicated by geological survey data (Masaitis, 1983) and recent studies. Within the Enisey-Khatanga basin the Permian-Triassic basalts are penetrated only by few wells (Vyssotski et al., 2006), but the volume of basalts under the Mesozoic – Cenozoic sedimentary cover is suggested to be significant. The synchronous manifestations of basaltic magmatism are found in the Pechora basin, the Chelyabinsk trough, Central Kazakhstan etc. (all located outside the limits of the Fig. 1A).

Within the Siberian platform the Permian-Triassic igneous rocks occur in the Tunguska syncline and its periphery, as well as along the northern boundary of the platform from the Norilsk region to the northern slope of the Anabar shield (Fig. 1A). The Siberian Traps province is conventionally divided into several regions according to the composition of igneous rocks and the tectonic structure of the area (e.g. Zolotukhin et al., 1986; Fedorenko and Czamanske, 1997). The most complete volcanic sections (up to 3–3.5 km of the total thickness) are located in the northern part of the platform in the Norilsk and Maymecha-Kotuy regions (Fedorenko and Czamanske, 1997). The central part of the Tunguska syncline is constituted by the thick pile of subhorizontal basalt flows. Finally, in the southern and eastern periphery

of the Tunguska syncline the Permian-Triassic Siberian Traps consist of tuffaceous deposits underlying the lava pile, and thick, mainly sill-like intrusions.

The recent paleomagnetic investigations of the Siberian Traps LIP were concerned about the thick volcanic sections of the Norilsk and Maymecha-Kotuy regions (Heunemann et al., 2004; Gurevitch et al., 2004; Pavlov et al., 2011a, 2015; Fetisova et al., 2014). Recently, the detailed results from the intrusive complexes have been published (Veselovskiy et al., 2012; Latyshev et al., 2013; Konstantinov et al., 2014). Despite these studies, until now there is a lack of modern reliable data for the volcanic sections of the central part of the Tunguska syncline and Putorana region, as well as for the intrusions from almost the entirety of the Tunguska syncline.

Our research included two profiles hundreds of km long that are stretched along the Nizhnyaya Tunguska (the western and central parts of the Tunguska syncline) and Chuna (the Angara-Taseeva depression, the southern part of the Siberian platform) rivers.

In the Chuna river valley we sampled 28 paleomagnetic sites from intrusions located in Ordovician – Silurian sediments. The sites are distributed over ~500 km along the Chuna river from Nizhneudinsk town near the platform margin to Octyabrskiy settlement in the central part of the Angara-Taseeva depression (Fig. 1B). The subhorizontally lying sills from 5 to 10 up to 150 m thickness prevail among the sampled intrusions. Dikes and stock-like bodies are less common but occur in several sites. The thick sills dominating in this area can be traced for hundreds of km. According to the published schemes of the Angara-Taseeva intrusions (Feoktistov, 1978; Ivanov et al., 2013), the Chuna river flows through the distribution area of the Tulunskiy, Padunskiy and Chuna-Biryusinskiy large sills. All studied intrusions are composed of dolerites, though the structure, size of crystals and the content of main rock-forming minerals depend on the position within the sill and can vary notably.

Sills in the sampling area of the Chuna river valley were dated by $^{40}Ar/^{39}Ar$ method (plagioclase) and yielded the ages of 241.9 ± 3.7/4.3 Ma (the middle reaches) and 241.6 ± 1.3/2.6 Ma (the upper reaches) (Ivanov et al., 2009), corresponding to the Middle Triassic. However, it should be noted that no U-Pb ages close to 240 Ma have been obtained from the Angara-Taseeva sills yet, whereas recent U-Pb data (CA-TIMS, zircon) for the Padunskiy sill vary in a range from 251.681 ± 0.063 Ma to 251.460 ± 0.051 Ma (Burgess and Bowring, 2015). Moreover, some large sills from the Angara-Taseeva depression, i.e. Padunskiy and Tolstomysovskiy sills, were dated using both U-Pb and $^{40}Ar/^{39}Ar$ methods, which yielded significantly different ages. However, paleomagnetic data indicates that intrusive units dated by different isotopic methods are coeval (Latyshev et al., 2013). This evidence indicates that the $^{40}Ar/^{39}Ar$ ages of the intrusions under investigation are ambiguous and need to be confirmed or disproved by U-Pb dating on the same localities. The full set of the available $^{40}Ar/^{39}Ar$ and U-Pb ages and the discussion of this data are presented at Section 6.5.

In the Nizhnyaya Tunguska river valley (the Tunguska syncline) we sampled 39 paleomagnetic sites from the Permian-Triassic intrusions between Tura settlement and the Nizhnyaya Tunguska river mouth (the distance between the endpoints reaches 1000 km). In addition, we collected samples from the volcanic section near Tura in 15 sites (Fig. 1C).

The volcanic section in the Nizhnyaya Tunguska river valley near Tura settlement (the central part of the Tunguska syncline) consists of 5 formations up to 2 km of aggregated thickness (Fig. 1D) (Ivanov et al., 2013). The lower Tutonchansky and Korvunchansky formations are mainly composed of volcaniclastic rocks; the upper Nidymsky, Kochechumsky and Yambukansky formations constitute the basaltic lava pile. Layers of sedimentary rocks of up to 15 m thickness were found in the Nidymsky and Kochechumsky formations, pointing out the prolonged gaps in the volcanic activity. The most part of the volcanic sequence except the lowermost Tutonchansky formation is considered to be the Early Triassic (Domyshev, 1974), though reliable isotopic data are scarce. The age of the sampled part of the volcanic pile and its correlation with other regions of the Siberian Traps LIP are discussed at Section 6.4–6.5.

According to the previous paleomagnetic data (Sidoras, 1984), the most part of the volcanic section has the normal polarity, though the reversely magnetized intervals were found in the lowermost Tutonchansky and uppermost Yambukansky formations. However, these results were obtained without using the modern paleomagnetic methods (e.g. principal component analysis (Kirschvink, 1980) was not performed); moreover, division of the lava pile into single flows is not presented in the cited work. Therefore, these paleomagnetic results require the confirmation by the up-to-date paleomagnetic techniques.

We collected paleomagnetic samples from 8 lava flows of the Nidymsky formation, 3 lava flows of the Kochechumsky formation and 4 sites of tuffaceous deposits referred to the Korvunchansky formation. Unfortunately, because of the fragmentary exposure the stratigraphic sequence of sampled units cannot be fully restored.

Intrusions from the Nizhnyaya Tunguska river are mainly sills. Dikes and stock-like bodies are rare. The majority of intrusions is composed of dolerites. The thickness of intrusions varies from few meters up to hundreds of meters, some bodies can be traced for dozens of km along strike. In the western part of the studied region intrusions are usually localized in Upper Paleozoic sediments of the Tunguska syncline, while in the eastern part they also cut Permian-Triassic tuffaceous deposits and basaltic lavas up to the Nidymsky formation. Furthermore, in the eastern part of the studied region there is a distinct group of the differentiated intrusions varying from dolerites to gabbro–syenites (4 paleomagnetic sites). Such intrusions are believed to be younger age and shown in the geological maps as cutting all volcanic sequence including the youngest lavas of the Yambukansky formation (though the geological relations in the field are not obvious in many cases due to poor exposure). For example, one of the sampled intrusions (site 13-12) is actually located in the Yambukansky Fm field, but the contacts are not exposed. Other intrusions cut the Korvunchansky and Nidymsky formations, and therefore their suggested younger age is uncertain.

The published U-Pb data from sills of the Nizhnyaya Tunguska river valley established their emplacement ages as Early Triassic: 251.795 ± 0.070 Ma and 251.786 ± 0.054 Ma – for the sills from the lower reaches of the Nizhnyaya Tunguska river; 251.74 ± 0.18 Ma – for the intrusion 150 km eastward from Tura settlement (CA-TIMS, zircon; Burgess and Bowring, 2015). The above-mentioned differentiated intrusions cutting the total volcanic section are suggested to be Middle Triassic according to the State Geological Map of Russia, but reliable isotopic data are not available for these intrusions.

3. Methods

Because of the vast lacunas in field exposure, it is not often possible to determine whether sampled sites represent different intrusions or the outcrops of a single body. In order to achieve a more continuous distribution of the sites in the studied territory, we kept the distance not < 5–10 km between adjacent sites. The paleomagnetic samples were taken as hand blocks or drill cores and oriented using a magnetic compass with a control for possible deflection of the compass needle due to the strongly magnetized rocks. Between 8 and 25 cores or hand blocks (usually 10–12) were collected from each site. The local magnetic declination was calculated using the IGRF model (12th generation, revised in 2014). The paleomagnetic procedures were performed in the paleomagnetic laboratories of Schmidt Institute of Physics of the Earth (IPE RAS, Moscow, Russia) and Lomonosov Moscow State University (MSU, Russia). All samples (cores or hand blocks) were subjected to the stepwise thermal treatment up to the complete demagnetization in 10–18 steps. The majority of samples were demagnetized up to 580–600 °C, in few cases – up to 645 °C. The size of demagnetization

steps was changed from 50 to 100 °C at low temperatures to 15–20 °C at high temperatures depending on the demagnetization pattern. For heating we used MMTD-80 non-magnetic ovens (Magnetic Measurements Ltd., Aughton, U.K.) with internal residual fields of about 5–10 nT. Several samples were demagnetized by alternating fields (AF) up to 130 mT with the AF-demagnetizer inbuilt in the 2G Enterprises cryogenic magnetometer. The remanent magnetization of samples was measured using the spinner magnetometers JR6 (AGICO, Brno, Czech Republic) at MSU and IPE RAS, and the 2G Enterprises cryogenic magnetometer "Khramov" at IPE RAS. The isolation of the natural remanent magnetization (NRM) components was performed with Remasoft (Chadima and Hrouda, 2006) or Enkin's (Enkin, 1994) paleomagnetic software packages using principal component analysis (Kirschvink, 1980). The analysis of paleomagnetic data was carried out using Fisher statistics (Fisher, 1953). Secular variation parameters were calculated using the program package PmagPy developed by Tauxe et al. (2016a). The rock-magnetic investigation was carried out in IPE RAS. Thermomagnetic Ms(T) curves were measured using magnetic balance constructed by Yu.K. Vinogradov (the Borok Geophysical Observatory, Yaroslavl region, Russia) in an applied magnetic field of 0.37 T. The hysteresis loops and back-field demagnetization curves of saturation IRM were recorded using vibrating sample magnetometer PMC MicroMag 3900 (Lake Shore Cryotronics, USA) at room temperature in a 0.5 T saturating field. The domain structure of ferromagnetic grains was determined according to the Day plot (Day et al., 1977).

4. Rock-magnetic properties

Thermomagnetic Ms(T) curves of samples from both Chuna and Nizhnyaya Tunguska rivers were recorded up to 650 °C and typically yielded Curie temperatures in the range of 500—580 °C, whereas for a couple of samples Curie points of ~450 °C were determined. Such Curie points indicate that magnetite and low-titanium titanomagnetite are the main carriers of the NRM (Fig. 2A, B).

The typical hysteresis loops and back-field curves are shown in Fig. 2C–D. The shape of hysteresis loops for samples both from the Chuna river and the Nizhnyaya Tunguska river are common for the magnetites or titanomagnetites of pseudo-single domain structure. The hysteresis parameters Mrs/Ms and Hcr/Hc for all samples from both localities vary within 0.05–0.3 and 1.6–3.5 respectively. These values lie in the pseudo-single domain region of the Day plot (Fig. 2E). The measured rock-magnetic properties are similar to those previously reported from lavas (e.g. Heunemann et al., 2004) and intrusions (Konstantinov et al., 2014) of the Siberian Traps LIP.

The detailed rock-magnetic and scanning electron microprobe investigation of dolerites from the Nizhnyaya Tunguska river was carried out in the Borok Geophysical Observatory (IPE RAS). Their results are presented in (Shcherbakov et al., 2017) and are generally consistent with our data. Briefly, magnetite and titanomagnetite, sometimes low-temperature oxidized, were identified as the main carriers of the remanence. Furthermore, the effect of partial self-reversal was detected in some samples. Some other peculiarities of the rock-magnetic properties of the Nizhnyaya Tunguska river intrusions are discussed below at Section 5.1, in relation to the components of remanence, while the complete description is reported in (Shcherbakov et al., 2017).

5. Paleomagnetism

5.1. The Nizhnyaya Tunguska river intrusions

The majority of samples from the studied intrusions, with the exception of the above-mentioned differentiated intrusions, demonstrate the excellent paleomagnetic record. In almost all sites we isolated the low-temperature component (LTC) destroyed at 200–300 °C. Since the directions of this component are close to the present geomagnetic field, we considered that the LTC has a viscous origin. Also the high-temperature component (HTC) generally unblocking in the range of 440–580 °C (in some cases from 300 to 615 °C) is clearly distinguished in all sites (Fig. 3A, B). The HTC has both normal (23 sites) and reversed polarity (12 sites) and its directions are close to those expected for the Permian-Triassic Siberian Traps LIP (e.g. Pavlov et al., 2007). In 16 sites out of 35 the HTC is the only isolated component except the viscous one (Fig. 3A).

In 14 sites we also distinguished the middle-temperature component (MTC), which demonstrates the directions virtually antipodal to those of the HTC (Fig. 3B). The unblocking temperature range of MTC varies in different sites from 240 to 450 °C to 400–540 °C and 530–590 °C. The number of samples carrying the MTC and the clarity of its manifestation vary from site to site, too. The MTC in different sites has both normal and reverse polarity as well as the HTC. Finally, in 6 sites the component virtually antipodal to the HTC was isolated at the highest temperatures (usually at 560–615 °C). This component (UHTC) is generally distinguished based on 2 or rarely 3 consequent steps of demagnetization (Fig. 3C).

Thirteen samples corresponding to the different component sets of the NRM were subjected to the stepwise demagnetization by alternating field. All studied samples showed 2-component constitution of the NRM vector (Fig. 3D). The low-coercive component is removed at fields about 5–10 mT and probably has viscous origin. The high-coercive component is usually destroyed at 10–80 mT and has the same polarity as HTC does in these samples. None of the samples showed the evidence of the antipodal components similar to the MTC or UHTC isolated after the thermal treatment.

Recently in the paper (Shcherbakov et al., 2017) authors presented the results of detailed thermomagnetic and microprobe investigations of the same samples with the MTC and math modeling. In particular, it was shown that the samples with the only HTC component are stable upon the successive heating in the saturation field, while the samples with the "anomalous" components demonstrate the changes of magnetic minerals. Authors explained the MTC appearance by the presence of self-reversing low-temperature oxidized titanomagnetites. As to the UHTC component, it could be the instrumental artifact or originate because of "…mineralogical changes in spinodal decomposition structures" during the stepwise heating, as suggested by (Shcherbakov et al., 2017).

Other possible explanations of the MTC and UHTC occurrence are the latter remagnetization or the successive record of different polarities during the slow cooling of intrusion. In our opinion, several arguments against remagnetization could be stated out. First, the studied dolerites do not demonstrate any evidence of the latter reheating. Only the weak low-temperature alteration was found in the intrusions. Furthermore, in none of the sites the direct contacts or cross-cutting relations of the different intrusions were observed, as well as the nearby location of two or more intrusive bodies. Finally, the MTC and UHTC usually appear not in all samples within the sites and are absent during the AF treatment. It is another argument that the occurrence of these components is not caused by the reheating, but is the result of magnetic mineralogy features.

As to the possible record of both polarities during the slow cooling, this phenomenon can occur during the cooling of large granitic plutons or the exhumation of metamorphic rocks (e.g. Rochette et al., 1992; Crouzet et al., 2001). The emplacement of the studied intrusions likely took place at shallow depth (some of them are located in the Permian-Triassic volcanic rocks), and the cooling time of even 100-m thick sills to the temperatures about 200–300 °C is estimated as first thousand years (Konstantinov et al., 2014). Since the duration of polarity chrons in the Early Triassic was about hundreds of thousand years (Hounslow and Muttoni, 2010), we consider the successive record of more than one polarity interval within the same intrusion to be unlikely.

In view of all foregoing arguments, we consider the HTC component as primary, and the MTC and UHTC are not discussed below. It should

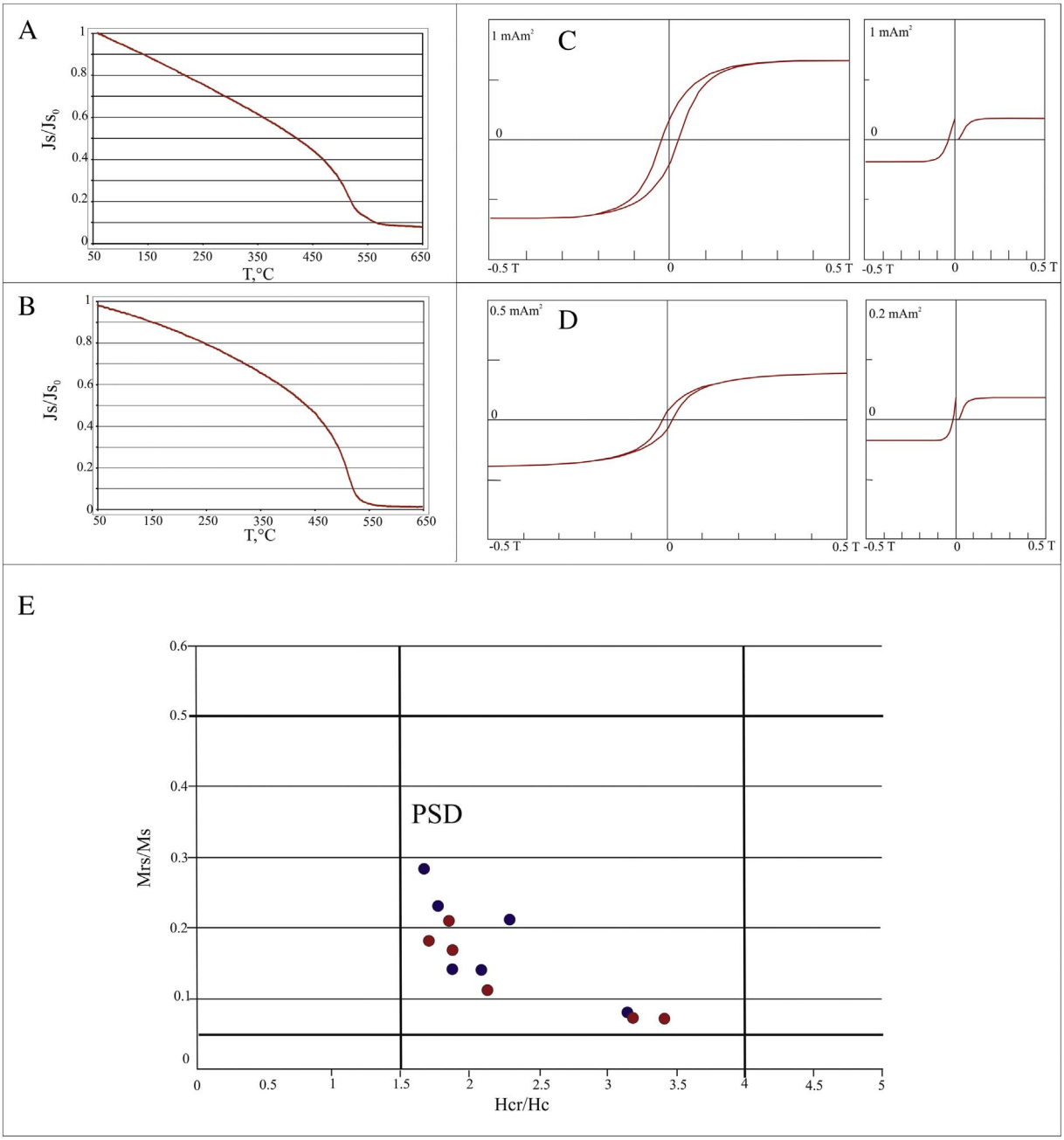

Fig. 2. Rock-magnetic properties of the studied samples. A–B. Thermomagnetic curves Ms(T). A – sample 72, site 7-14, Nizhnyaya Tunguska. B – sample 103, site 8-15, Chuna. C-D – Typical hysteresis plots (left) and back-field curves (right). C – sample 136, site 10-15, Chuna. D – sample 228, site 21-4, Nizhnyaya Tunguska. E – Day plot (Day et al., 1977). Ms – saturation magnetization; Ms_0 – saturation magnetization at room temperature; T – temperature, °C; PSD – pseudo-single domain field; the Hysteresis parameters: Ms – induced saturation magnetization; Mrs – remanent magnetization after saturation; Hc – coercitivity; Hcr – coercivity of remanence. Blue circles mark the samples from the Chuna river, red circles – from the Nizhnyaya Tunguska river. (For interpretation of the references to color in this figure legend, the reader is referred to the web version of this article.)

be noted that even if widely occurred MTC is the result of the overprint in some sites, it would not influence our assumption. All further calculations are carried out using the HTC directions. The site-mean directions are shown in Table 1.

In the samples from the differentiated intrusions (4 sites) the quality of paleomagnetic signal varies from satisfying to completely unreliable. By “satisfying quality” we mean the paleomagnetic signal, suitable for the stable component of NRM isolation, with the maximum angular deviation (MAD) > 6°. In the case of completely unreliable record we were not able to isolate any stable components. Nevertheless, we managed to calculate the mean directions for all sampled differentiated intrusive bodies. The unblocking temperatures of the characteristic component of NRM vary from 300 to 470 °C to 500–620 °C. All four intrusions demonstrate the reversed polarity and have flatter inclinations comparing to dolerites from the main group. The mean directions for these intrusions are shown in Table 1. Because of the noisy paleomagnetic signal, distinct paleomagnetic directions from the other intrusions and possible essentially younger age (the Middle Triassic?) we excluded the results for these sites from the further calculations.

5.2. The Chuna river intrusions

The paleomagnetic record is clear in the majority of studied samples. In all sites the low-temperature (LTC) and high-temperature (HTC) components were isolated. The LTC is destroyed at 200–350 °C, is virtually close to the present geomagnetic field direction and probably has

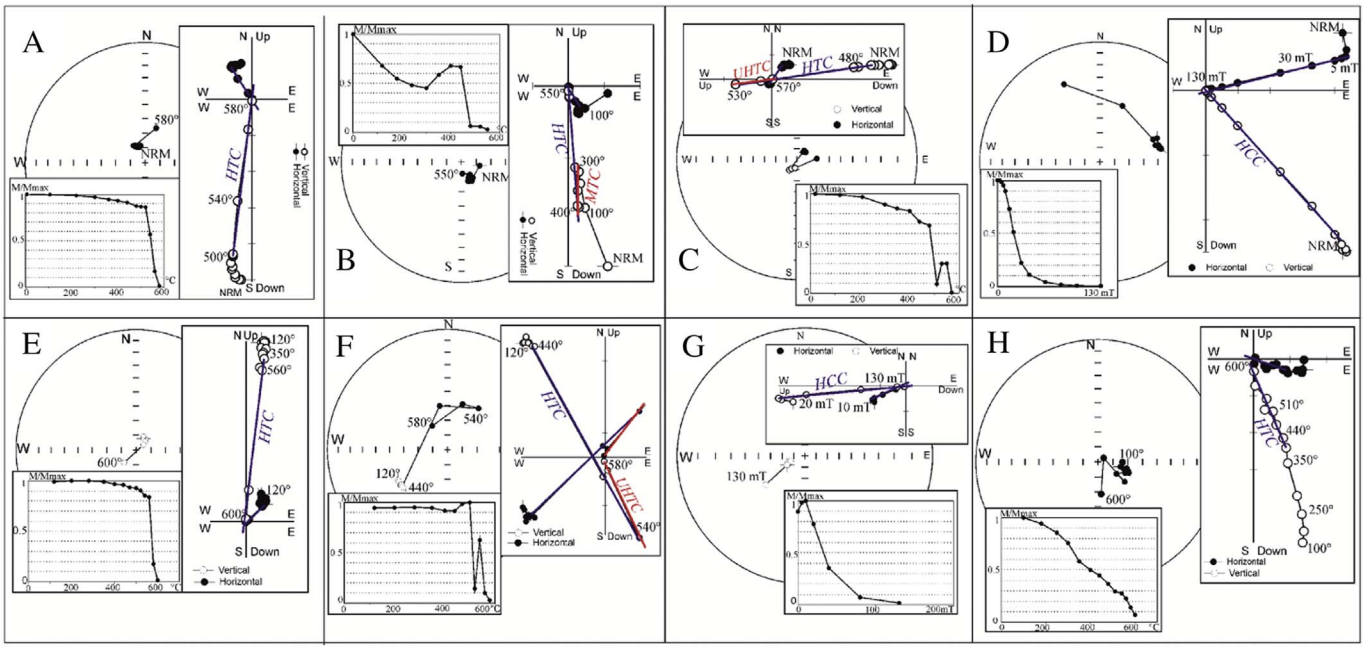

Fig. 3. Results of the stepwise thermal and AF demagnetization (geographic coordinate system). A – sample 225, site 21-14, the Nizhnyaya Tunguska river; HTC is isolated at 480–580 °C. B – sample 22, site 3-14, the Nizhnyaya Tunguska river; HTC is isolated at 400–550 °C; MTC is isolated at 300–400 °C. C – sample 268, site 25-14, the Nizhnyaya Tunguska river; HTC is isolated at 440–530 °C; UHTC is isolated at 530–570 °C. D – sample 361, site 34-14, the Nizhnyaya Tunguska river; high-coercive component is isolated at 10–130 mT. E – sample 99, site 7–15, the Chuna river; HTC is isolated at 500–600 °C. F – sample 123, site 9-15, the Chuna river; HTC is isolated at 440–540 °C; UHTC is isolated at 540–580 °C. G – sample 301, site 19-15, the Chuna river; high-coercive component is isolated at 10–130 mT. H – sample 179, site koch 2, Kochechumsky Formation, the Nizhnyaya Tunguska river; HTC is isolated at 400–600 °C.

the viscous origin. The manifestations of the HTC occur from 280 to 615 °C, in most cases it is unblocked in the range of 470–580 °C (Fig. 3E) and in all sites the HTC has the reversed polarity. Besides, in 3 sites the middle-temperature component is distinguished at temperatures of 300–480 °C. In two sites the HTC and MTC directions are approximately antipodal and in one site the MTC directions are widely scattered. Finally, in few samples from 8 sites at 560–600 °C we found the traces of the component similar to the UHTC isolated in the Nizhnyaya Tunguska river intrusions. This component is recorded by 2 or rarely 3 consequent steps of demagnetization and is antipodal to the HTC (Fig. 3F).

We subjected 11 samples from sites with the various component constitutions to the AF-demagnetization. All samples demonstrated the high-coercive component of reversed polarity unblocking at 5–80 mT. The directions of this component were close to those of HTC from the same sites (Fig. 3G). No evidence of the antipodal components similar to the MTC and UHTC were found in the studied samples. Since the unblocking temperatures and manifestation features of the MTC and UHTC in the Chuna river intrusions are similar to those from the Nizhnyaya Tunguska river intrusions, we used only the HTC component in our further calculations.

The site-mean directions were calculated for all sites except two where the distribution of directions is irregular. The results are presented in Table 2.

5.3. Lava flows and tuffaceous deposits of the Tunguska syncline

The basalts from the Nidymsky and Kochechumsky formations usually demonstrate good paleomagnetic record with clearly distinguished components or moderate paleomagnetic signal, when directions are isolated but have greater errors (MAD > 6 °). Besides the low-temperature viscous component, the majority of demagnetized samples have the single high-temperature component of NRM. The unblocking temperature range of this component varies from 300 to 500 °C to 400–590 °C in different flows (Fig. 3H). All 11 sites of lavas yielded mean paleomagnetic directions of only normal polarity in agreement with previously reported results for the same lava section (Pan et al., 2013).

The most part of the Korvunchansky tuff samples shows the noisy and hardly distinguishable paleomagnetic signal. Only for one site out of four we managed to obtain the mean direction using at least 5 samples. The characteristic component of magnetization in this site has the normal polarity and is unblocked at 440–640 °C.

The results of the thermal demagnetization of samples from the Nidymsky, Kochechumsky and Korvunchansky formations are presented in Table 3.

6. Discussion

6.1. The Nizhnyaya Tunguska river intrusions

As shown previously, the sampled dolerite intrusions have both normal and reversed polarity (Fig. 4A). The reversal test (McFadden and McElhinny, 1990) performed for the mean directions of the normally and reversely magnetized sites (except the differentiated intrusions) is positive: γ/γ_{cr} = 0.4°/6.0°. It should be noted, that since the sampled objects are spread over 1000 km along the Nizhnyaya Tunguska river, all paleomagnetic directions, used for the comparison, are recalculated to the middle point (64.6°N; 94.4°E), using the VGP method (Irving, 1964). We calculated the geographical coordinates of the VGP from the site values of declination and inclination, and then the corresponding direction of the middle point using the geocentric dipole hypothesis. Positive reversal test argues, firstly, in favor of the primary origin of the NRM in studied samples and, secondly, for the averaging of the geomagnetic field secular variations recorded during the intrusions emplacement.

We also calculated the mean pole for the Nizhnyaya Tunguska river intrusions ("NT": N = 35; Plong = 133.6°; Plat = 56.2°; B95 = 5.0°) and compared it with the paleomagnetic "Siberian Traps" pole NMK (Pavlov et al., 2011b) obtained from the most complete lava sections of

Table 1
The site-mean directions for the Nizhnyaya Tunguska river intrusions.

Site	slat	slong	n/n$_0$	D,°	I,°	K	α95
Dolerite intrusions							
1–14	N63°49.521′	E97°56.489′	10/10	123.1	80.9	353.9	2.6
2–14	N63°44.259′	E97°59.551′	10/11	66.1	77.6	70.6	5.8
3–14	N63°47.014′	E97°24.310′	10/10	166.2	82.4	361.9	2.5
4–14	N63°47.815′	E96°38.953′	10/10	130.3	79.3	539.9	2.1
9–14	N64°11.131′	E94°36.270′	12/12	71.3	81.6	500.5	1.9
10–14	N64°10.560′	E94°20.703′	10/10	95.6	81.3	746.4	1.8
11–14	N64°10.745′	E93°50.364′	10/10	109.9	67.5	272	2.9
13–14	N64°21.447′	E93°14.543′	9/9	95.2	70.7	125.3	4.6
14–14	N64°25.921′	E92°56.059′	13/13	80.8	72.7	189	3
15–14	N64°22.989′	E92°38.102′	11/11	133	77.0	375.7	2.4
18–14	N64°25.827′	E91°52.121′	9/9	93.7	81.7	239.8	3.3
21–14	N64°35.242′	E90°56.030′	11/11	142.6	74.7	498	2
22–14	N64°44.233′	E90°43.697′	10/11	89.0	78.5	57.8	6.4
25–14	N65°01.488′	E90°12.754′	11/11	82.6	81.6	95.4	4.7
26–14	N65°04.812′	E90°05.154′	11/12	29.4	76.1	50.6	6.5
27–14	N65°09.281′	E89°59.598′	8/10	50.0	70.6	39.7	8.9
28–14	N65°16.427′	E89°59.116′	10/11	112.0	83.0	51.1	6.8
29–14	N65°27.502′	E89°58.374′	10/10	141.5	71.6	408.9	2.4
31–14	N65°36.068′	E90°03.950′	8/11	69.5	75.2	60.7	7.2
32–14	N65°41.520′	E89°48.470′	11/11	105.9	63.6	67.5	5.6
34–14	N65°50.833′	E89°15.676′	11/11	70.7	75.8	179.3	3.4
15–12	N64°06.453	E98°05.093′	6/9	39.1	83.4	23.2	14.2
11–12	N64°16.440′	E100°14.595′	6/8	42.6	78.6	42.3	10.4
5–14	N63°53.402′	E95°54.618′	12/12	300.8	−77.0	165.8	3.4
6–14	N63°55.945′	E95°47.643′	10/11	301.5	−71.9	232.3	3.2
7–14	N64°01.020′	E95°21.791′	10/10	259.4	−74.9	513.3	2.1
12–14	N64°15.055′	E93°33.203′	10/11	216	−66.8	289	2.8
16–14	N64°21.528′	E92°19.075′	11/11	322.4	−65.8	355.1	2.4
17–14	N64°20.476′	E92°09.700′	9/10	285.2	−76.0	407.5	2.6
19–14	N64°27.741′	E91°24.049′	10/10	284.8	−77.8	113.7	4.6
20–14	N64°31.394′	E91°10.304′	11/11	300.9	−80.6	125.7	4.1
23–14	N64°46.226′	E90°36.339′	9/11	261.2	−84.2	101.5	5.1
24–14	N64°54.476′	E90°17.857′	11/11	273	−79.7	508.9	2
30–14	N65°32.321′	E90°00.169′	11/11	260.9	−80.0	272.5	2.8
33–14	N65°45.487′	E89°30.920′	11/11	210.7	−76.1	42.2	7.1
Differentiated intrusions							
13–12	N64°17.221′	E99°08.279′	12/22	227.1	−57.2	7.8	16.6
6–12	N64°07.049′	E101°12.039′	5/7	229.1	−66.9	30	14.2
4–12	N64°02.358′	E102°18.381′	22/22	250.8	−62	47.8	4.5
3–12	N64°01.450′	E102°21.376′	33/39	260.1	−67.3	20.6	5.6

n/n$_0$ – number of samples used in the calculation/total number; D – declination; I – inclination; K, α95 – Fisher statistic parameters; Slat, slong – the site coordinates.

the Norilsk and Maymecha-Kotuy regions. These poles are not identical, but close to each other, and their 95%-confidence circles overlap (Fig. 4B). This fact also favors that secular variations are adequately averaged. The moderate values of K parameter (the concentration parameter in Fisher statistics) confirm this suggestion too (K = 82.7 for the site-mean direction for the normal polarity and K = 62.0 for the reversed polarity). Generally, we could not distinguish any representative tight clusters of directions, which would correspond to the brief and intense magmatic events, similar to those reported by Latyshev et al. (2013) and Konstantinov et al. (2014) for the intrusions from southern and eastern periphery of the Siberian Traps LIP, respectively.

The distribution of site-mean virtual geomagnetic poles (VGP) shown in Fig. 4B demonstrates almost circularly symmetrical shape (without the differentiated intrusions). This feature of VGP distribution used to be attributed to the units which were magnetized during more or less prolonged time period (e.g. Beck, 1999), suggesting that the secular variations are averaged. However, the recent analyses of the representative data sets from the lava sequences yielded the significant variability of elongation both for directions and poles (Bazhenov et al., 2016). It should be also noted that our directions sets both for normal and reverse polarities are visibly elongated (Fig. 4A), but it could be partly caused by the large area of sampling (hundreds of km along the Nizhnyaya Tunguska river).

Table 2
The site-mean directions for the Chuna river intrusions.

Site	slat	slong	n/n$_0$	D,°	I,°	K	α95
Location "Uda"							
8–15	N55°23.894	E99°25.703′	14/16	277.3	−62.7	121.9	3.6
9–15	N55°26.210′	E99°24.149′	13/14	265.1	−62.2	163.2	3.3
10–15	N55°28.745′	E99°25.040′	13/13	257.6	−61.8	103.5	4.1
11–15	N55°31.699′	E99°24.198′	10/11	262	−61	43.7	7.4
12–15	N55°33.977′	E99°29.189′	15/16	264.8	−62.1	181.8	2.8
13–15	N55°44.989′	E99°31.703′	8/14	263.8	−60.3	66.2	6.9
15–15	N55°52.443′	E99°33.105′	21/22	261.9	−63.2	39.3	5.1
Location "Chuna"							
18–15	N56°42.429′	E99°02.740′	12/12	262.8	−79.3	133.9	3.8
19–15	N56°43.619′	E99°02.773′	13/13	245.2	−81.2	83.8	4.6
20–15	N56°44.487′	E99°02.704′	12/12	236.9	−72.8	41.7	6.8
21–15	N56°53.035′	E99°03.081′	12/13	273.7	−75.1	138	3.7
22–15	N56°57.421′	E98°51.392′	5/12	244.2	−79.4	176	5.8
23–15	N56°59.912′	E98°48.554′	14/14	250.5	−80.5	61.8	5.1
24–15	N57°02.650′	E98°43.502′	11/11	245.2	−80.2	175.4	3.5
25–15	N57°02.991′	E98°38.888′	8/12	277.7	−81.6	77.7	6.3
27–15	N57°06.147′	E98°42.218′	13/13	222.3	−82	53.5	5.7
29–15	N57°10.004′	E98°24.165′	5/13	257.9	−82.5	51	10.8
"Nizhneudinsk-Octyabrskiy" group							
1–15	N55°01.073′	E98°58.550′	12/12	258.1	−75	69.6	5.2
2–15	N55°00.884′	E99°04.011′	13/13	267.4	−71.4	192	3
3–15	N55°09.534′	E99°05.557′	12/12	284.8	−72	104.8	4.3
5–15	N55°11.959′	E99°23.814′	10/12	274.7	−68.1	21.8	10.6
7–15	N55°20.907′	E99°25.165′	11/11	336	−73.1	19.5	10.6
28–15	N57°09.510′	E98°24.765′	13/13	221.3	−70.5	104.9	4.1
30–15	N57°25.859′	E97°47.453′	13/13	274	−65.4	131.3	3.6
31–15	N57°25.539′	E97°45.099′	13/16	293.9	−68.5	86.4	4.5
32–15	N57°24.709′	E97°35.739′	8/13	227.8	−56.7	47.6	8.1
Padunskiy sill, Angara (from Latyshev et al., 2013)							
a21–1	N56°05′01.7″	E101°12′19.8″	8/8	280.6	−82	129.6	4.9
a21–2	N56°05′01.7″	E101°12′19.8″	6/8	263.7	−80.5	74.5	7.8
A26	N56°17′34.3″	E101°48′30.8″	11/12	277.2	−76.3	111.6	4.3
A27	N56°17′15.3″	E101°47′51.0″	10/11	255.6	−76.7	65.1	6.0
A28	N56°17′20.6″	E101°48′01.7″	9/10	255.1	−78.7	79.1	5.8
a18	N56°04.849′	E101°43.352′	12/13	282.2	−78.5	97.5	4.4
a19	N56°07′23.3″	E101°24′07.5″	11/12	318.3	−77.8	107.8	4.4
Tulunskiy sill, Angara (from Latyshev et al., 2013)							
a22–2	N55°30′52.4″	E101°42′11.5″	5/8	259.4	−59.2	93.6	8
a22–3	N55°30′52.4″	E101°42′11.5″	5/8	260.7	−61.8	392.8	3.9
a22–4	N55°30′52.4″	E101°42′11.5″	6/8	287.6	−71.3	110.2	6.4
a23–1	N54°34′20.5″	E100°35′29.0″	10/13	286.4	−66.8	21	10.8
a23–2	N54°34′20.5″	E100°35′29.0″	10/12	280.3	−62	100.7	4.8
a24–1	N54°35′14.9″	E100°47′45.9″	6/8	253.8	−47.2	48.5	9.7
a24–2	N54°35′14.9″	E100°47′45.9″	6/8	246.7	−62.4	77.6	7.7
a24–3	N54°35′14.9″	E100°47′45.9″	6/8	250.3	−65.9	110.2	6.4
a24–4	N54°35′14.9″	E100°47′45.9″	6/8	263.1	−63	177.1	5

n/n$_0$ – number of samples used in the calculation/total number; D – declination; I – inclination; K, α95 – Fisher statistic parameters; Slat, slong – the site coordinates.

Table 3
The site-mean directions for the volcanic section near Tura.

Site	Slat	Slong	n/n$_0$	D,°	I,°	K	α95
Tuffs	N64°10.154′	E98°14.199′	7/8	79.1	77.3	69.5	7.3
koch1	N64°18.018′	E100°20.493′	6/15	344.2	77.1	22.8	14.3
koch2	N64°17.959	E100°19.933′	6/7	112.4	78.8	26.8	13.2
koch3	N64°17.946	E100°19.493	7/8	39.9	80.2	81.3	6.7
nidym1	N64°07.049′	E101°12.039′	6/11	169.9	54	23.3	14.2
nidym2	N64°17.217′	E100°17.620′	8/12	82.2	75.3	60.5	7.2
nidym3	N64°16.057′	E100°13.303′	9/10	128.5	66.4	25.1	10.5
nidym4	N64°16.057′	E100°13.303′	15/16	116.6	71.6	45.9	5.7
nidym5	N64°11.425′	E99°58.050′	6/8	150.2	70.2	65.2	8.4
nidym6	N64°11.425′	E99°58.050′	4/8	113.6	67.9	70.2	11
nidym7	N64°08.821′	E99°13.338′	8/8	127.5	68.2	158.9	4.4
nidym8	N64°08.821′	E99°13.338′	5/8	139.7	70.7	212.8	5.3

n/n$_0$ – number of samples used in the calculation/total number; D – declination; I – inclination; K, α95 – Fisher statistic parameters; Slat, slong – the site coordinates.

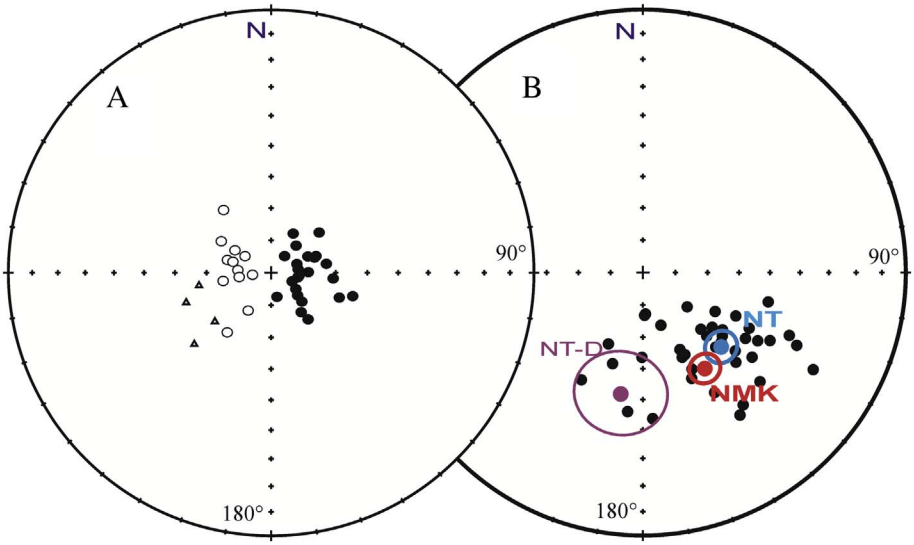

Fig. 4. Results of the paleomagnetic investigation of the Nizhnyaya Tunguska river intrusions (geographic coordinate system).
A. The site-mean directions of the studied intrusions. Black circles mark the normal polarity; unfilled circles – reversed polarity, unfilled triangles – differentiated intrusions (reversed polarity).
B. VGP distribution and mean poles for the Nizhnyaya Tunguska river intrusions. NT - mean pole for dolerite intrusions of the Nizhnyaya Tunguska river (N + R polarity); NMK - "Siberian Traps" paleomagnetic pole (Pavlov et al., 2011b); NT-D – mean pole for the differentiated intrusions.

The mean pole calculated for 4 differentiated intrusions is clearly different from both NT and NMK poles. It could be explained by the actually younger age of these intrusions as suggested by the geological survey or by the briefness of this intrusive event and, consequently, non-averaging of the secular variations. However, paleomagnetic data for this group of intrusions is too scarce to choose any explanation confidently.

6.2. The Angara-Taseeva depression intrusions

The mean paleomagnetic directions of the reverse polarity were calculated for 26 sites along the Chuna river. Nevertheless, the distribution of directions demonstrates at least two clearly distinguishable clusters correlating with the geographic location of sites. Though incomplete exposure did not allow us to find the contacts of discrete intrusions, sites with close paleomagnetic directions are lined up along the Chuna river valley. Considering these two factors (geographic location and paleomagnetic directions), we divided all studied sites into 3 groups (Fig. 5A, Table 2):

- The group of sites with western declinations (D = 257–277°) and flatter inclinations compared with group 2 ($I = -60\ldots-63°$). This group includes 7 site-mean directions from successively located sites in the upper reaches of the Chuna river (sites 8-15–15-15 – location "Uda").
- The group of sites with western and southwestern declinations (D = 222–277°) and steep inclinations ($I = -75\ldots-82°$). This cluster contains 10 site-mean directions from sites in the middle reaches of the Chuna river (sites 18-15 – 29-15 – location "Chuna").
- Nine remaining site-mean directions which are intermediate between the two distinguished groups (sites 1-15 – 5-15, 30-15 – 31-15) or significantly distinct from the main bulk of directions (sites 7-15, 32-15, 28-15) were nominally combined into the group 3. These sites represent sills near Nizhneudinsk town (sites 1-15 – 7-15) and Octyabrskiy settlement (sites 28-15 - 32-15), i.e. they are located either upstream or downstream from the other sites along the Chuna river (group "Nizhneudinsk-Octyabrskiy").

We calculated the mean virtual geomagnetic poles (VGP) for the directional groups (DG) "Uda" and "Chuna" and compared them with VGPs, obtained for the large reversely magnetized Padunskiy and Tulunskiy sills from the Angara river valley (Latyshev et al., 2013; Table 2). The VGP distribution (Fig. 5B) reveals two tight clusters; the first of them corresponds to the Tulunskiy sill and "Uda" group and appears to be slightly elongate, and the second one includes VGPs of the Padunskiy sill and "Chuna" group, displaying the "loop-like" morphology. Other VGPs referred to "Nizhneudinsk-Octyabrskiy" group are rather scattered and do not show any regular pattern. This character of VGP distribution is clearly distinct from the Nizhnyaya Tunguska river intrusions.

The mean VGPs of the Tulunskiy sill and "Uda" group as well as the Padunskiy sill and "Chuna" group are statistically indistinguishable. Since the VGPs for all objects were calculated from not < 6 sites with high values of the concentration parameter K between sites, the coincidence of VGPs likely indicates that magmatic events are coeval.

Thus, it can be assumed that products of two voluminous magmatic events, resulted in emplacement of the Padunskiy and Tulunskiy sills as well as the associated intrusions, covered the vast area within the Angara-Taseeva depression (the Angara and Chuna rivers valleys). The distance between the endpoints where manifestations of these events are found exceeds 200 km (see Fig. 1B). In the previous study (Latyshev et al., 2013), another peak of voluminous intrusive magmatic activity was revealed for the northeastern part of the Angara-Taseeva depression - so-called "Tolstomysovskiy sill".

It should be emphasized that we have not enough data to claim that all sites belonging to the same directional group actually represent the same huge sill. On the contrary, our field data rather discovers separate small sills (e.g. site 8-15) and dikes (e.g. site 13-15). However, these intrusions can represent the branches or apophyses of the nearby thick sill. Therefore, here and below, when referring to "Padunskiy" or "Tulunskiy" sill etc., we mean an aggregate of spatially and genetically related intrusions combined into one group and marked the uniform magmatic event.

The sills near Nizhneudinsk and Octyabrskiy constituting the group 3 likely represent the magmatic event or events non-related to those responsible for the groups 1 and 2 formation. Since paleomagnetic directions for the sites from both these locations are close, there is a possibility that these intrusions are coeval. However, substantially more scattered paleomagnetic directions comparing with DG 1 and 2 and the absence of evident geological relations force us to take into account the chance of random coincidence of paleomagnetic directions.

When regarding the directional groups, we should discuss the possible remagnetization of the part of intrusions by the younger magmatic events. The arguments against remagnetization for the intrusions of the Angara-Taseeva depression are similar to those for the Nizhnyaya Tunguska river (see Section 5.1); besides, the positive contact tests reported for the Ordovician sediments in the proximity of the large Tolstomysovskiy sill (Pavlov et al., 2012; Latyshev et al., 2013) favor

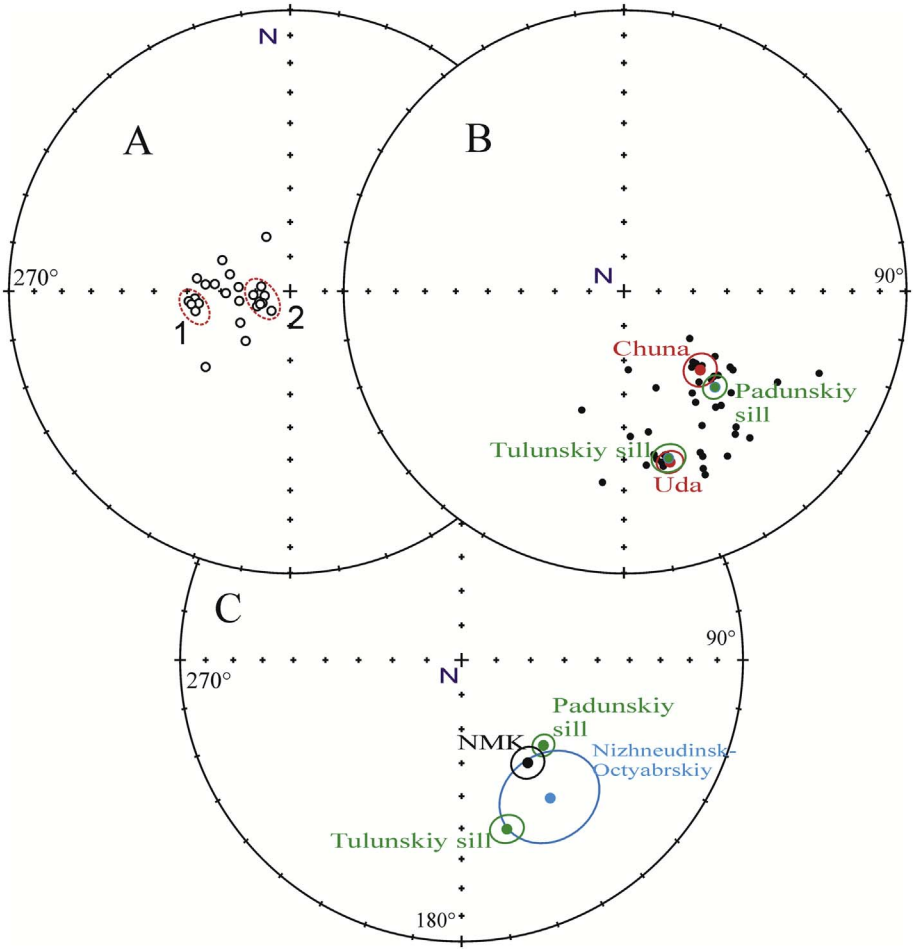

Fig. 5. Results of the paleomagnetic investigation of the Chuna river intrusions and their comparison with the data from the Angara river valley (geographic coordinate system).
A. Site-mean paleomagnetic directions for the Chuna river intrusions. 1 – DG "Uda"; 2 – DG "Chuna".
B. VGP distribution and mean poles for the Chuna directional groups (red) and sills from the Angara river (green).
C. Mean poles for the directional groups of the Angara–Taseeva depression and their comparison with the "Siberian Traps" pole NMK (Pavlov et al., 2011b). (For interpretation of the references to color in this figure legend, the reader is referred to the web version of this article.)

the absence of the regional reheating. The presence of the directional groups with the statistically different directions can be the additional argument against the regional overprint. Although we cannot completely exclude the possibility of the remagnetization of occasional sites, even in this case it means that the discussed magmatic event took place in this area.

The mean directions for distinguished DGs including the data from both the Chuna and the Angara rivers demonstrate the extremely tight clustering: K = 359.8 for the "Padunskiy sill" and K = 123.8 for the "Tulunskiy sill" (see Table 4; all directions are recalculated to the middle point (56.8°N; 99.4°E) using the VGP method). It can be interpreted in two ways:

1) Each out of two groups was formed during the geologically brief magmatic event. That resulted in non-averaging of the secular variations and extra tight grouping (Latyshev et al., 2013; Konstantinov

Table 4
The mean directions and poles for the studied objects.

Object	Mean directions					Poles		
	N	D,°	I,°	K	α95	Plong	Plat	A95
The Nizhnyaya Tunguska river[a]								
Mean for the normal polarity	23	95.1	79.2	82.7	3.3	133.5	56.5	6.1
Mean for the reverse polarity[b]	12	276.5	− 78.9	62	5.6	133.8	55.6	9.9
Differentiated intrusions	4	237.7	− 61.3	97.5	9.4	190.4	51.2	13.7
Mean for the normal and reverse polarity[b]	35	95.6	79.1	76.7	2.8	133.6	56.2	5
The Angara-Taseeva depression[c]								
Tulunskiy sill	16	264.1	− 62.3	123.8	3.3	165	37.8	4.6
Padunskiy sill	16	258.3	− 79.5	359.8	1.9	136.2	55.4	3.6
Nizhneudinsk-Octyabrskiy group	9	269.1	− 71.8	40	8.2	149.1	44.5	13.8
Lavas near Tura	12	122.6	75.8	32	7.8	132.8	45.5	13.4
The "Trap" pole NMK for the Permian-Triassic boundary on the Siberian platform (Pavlov et al., 2011b)						147.2	54.2	4.7
The normal polarity interval from Norilsk volcanic section (Pavlov et al., 2011a)						142.2	56.5	7.8

N – number of sites; D – declination; I – inclination; K, α95 – Fisher statistic parameters. Plat; Plong – latitude and longitude of the virtual geomagnetic pole.
[a] All directions are recalculated to the mean geographic point: N = 64.6°; E = 94.4°.
[b] Without differentiated intrusions.
[c] All directions are recalculated to the mean geographic point: N = 56.8° E = 99.4°.

et al., 2014).

2) On the contrary, the secular variations are averaged for each site individually as a result of the prolonged cooling of intrusions during the period sufficient for averaging of the secular variations.

Admitting the second explanation, we would suppose the slow continuous cooling of all sampled sites including thin dikes and sills or contact zones of large sills, which seems hardly possible. The presence of two such groups of intrusions with significantly different directions seems to be even more doubtful. Hence, we interpret extra tight clustering within the DGs from the Angara-Taseeva sills as a result of very rapid emplacement of these intrusions. As to the DG "Nizhneudinsk-Octyabrskiy", we suggest that it corresponds to the prolonged magmatic activity or series of the discrete local magmatic events, resulted in the scattered distribution of the site-mean directions.

The mean pole calculated for the Tulunskiy sill is clearly distinct from the paleomagnetic pole NMK (Fig. 5C) (Pavlov et al., 2011b). It could be explained in two ways: 1) very short magmatic event or 2) significantly younger age of the Tulunskiy sill than the Permian-Triassic boundary (as suggested by $^{40}Ar/^{39}Ar$ ages, Ivanov et al., 2009). The first explanation is consistent with our paleomagnetic data; the second version is discussed below (see Section 6.5).

The mean pole for Padunskiy sill is close to the NMK pole and their 95%-confident circles overlap (Fig. 5C). However, that is not enough to claim that the secular variations are averaged (see Section 6.3). As for the mean pole of the "Nizhneudinsk-Octyabrskiy" group, its confidence circle overlaps those for all shown mean poles due to high A95 ratio (13.8°), and the low precision does not allow to use this pole for any geological correlations.

6.3. The estimation of the secular variations amplitude

The obtained paleomagnetic data from the Padunskiy and Tulunskiy sills and the Nizhnyaya Tunguska river intrusions allowed us to estimate the amplitude of the secular variations during the emplacement of these magmatic complexes. We calculated the VGP scatter S_f according to (McElhinny and McFadden, 1997) for each group individually (see Table 5) and compared the results with the TK03 model of the secular variations of the geomagnetic field (Tauxe and Kent, 2004).

As shown in Fig. 6, the VGP scatters for the Padunskiy and Tulunskiy sills are significantly lower than expected according to the model TK03. As to the Nizhnyaya Tunguska river intrusions, the value of S_f is somewhat lower than expected, but the upper extremity of the confidence interval overlaps the model curve.

The previous paleomagnetic investigation of the volcanic sections from the Norilsk and Maymecha-Kotuy regions provided the strong evidence that the amplitude of the secular variations of the geomagnetic field on the Permian-Triassic boundary was close to that in the Late Cenozoic (Pavlov et al., 2011a). Thereby, we explain the low secular variations amplitude for the Padunskiy and Tulunskiy sills as a result of insufficient averaging of secular variations due to rapid emplacement of these magmatic bodies. If so, then the proximity of the mean pole for the Padunskiy sill to the NMK pole is with a high probability just a coincidence. The duration of the magmatic events resulted in emplacement of the Padunskiy and Tulunskiy sills and associated intrusions could be estimated as not succeeding 10–100 kyr, according to the modern evaluations of the period sufficient for the variations averaging (Tauxe et al., 2016b).

Table 5
Parameters of the geomagnetic field secular variations.

Object	N	Sf,°	Sfmin	Sfmax
The Nizhnyaya Tunguska river intrusions	35	16.6	13.6	19.3
Padunskiy sill	16	7.9	5.9	9.6
Tulunskiy sill	16	10	6.6	12.9

N – number of sites; Sf – VGP scatter according to (McElhinny and McFadden, 1997); Sfmin – Sfmax – confidence interval.

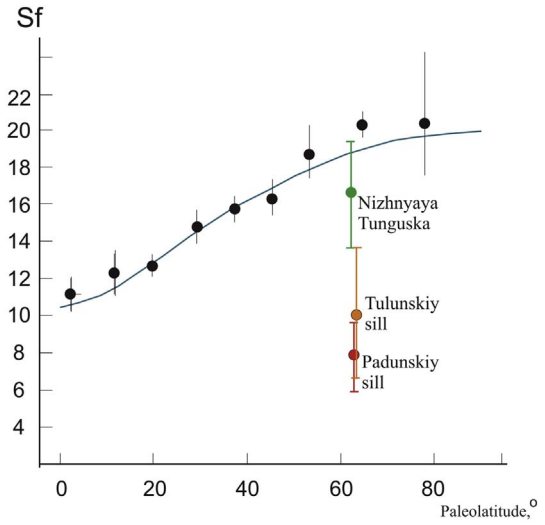

Fig. 6. The scatter of VGPs and its comparison with the model TK03 (Tauxe and Kent, 2004). Estimated latitude dependence of VGPs scatter from data compilation of McElhinny and McFadden (1997) (black dots). Blue line is the predicted dependence from model TK03 (Tauxe and Kent, 2004). (For interpretation of the references to color in this figure legend, the reader is referred to the web version of this article.)

In spite of the relatively low amplitude of the secular variations recorded in the Nizhnyaya Tunguska river intrusions, we suggest that their formation was more even and took the longer time compared with the Angara-Taseeva intrusive complexes. This is confirmed by the presence of both normal and reversed polarity in the studied objects, the positive reversal test and the overlapping of the confidence intervals of the poles NMK and NT (see Section 6.1).

The difference of the shapes of VGP distributions for two regions is an additional sign of the different styles of the magmatic activity. While the VGP set of the Nizhnyaya Tunguska river intrusions demonstrates almost circular shape, the distribution of VGPs from the Angara-Taseeva depression is clearly non-Fisherian. We suggest that the observed tight clusters, either elongate or containing loops and kinks, provide an extra argument that secular variations were not averaged during the corresponding magmatic events.

In addition, we compared our data with the geomagnetic field variations recorded in thick volcanic sections. The compilation of the secular variations data from pre-Late Cenozoic lava sequences, suggested to average the geomagnetic field, was composed by (Bazhenov et al., 2016). Comparing the concentration parameters (K) values of the Padunskiy and Tulunskiy sill groups ($K = 359.8$ and $K = 123.8$ respectively) with those from the lava sections, it is clearly seen that our directional groups from the Angara-Taseeva intrusions are much more tightly clustered than lava series included in the compilation (where $K < 100$ for all cases). As to the Nizhnyaya Tunguska river intrusions, the concentration parameter values ($K = 82.7$ for normal polarity and $K = 62.0$ for the reversed polarity) are higher than those for the majority of lava series – see (Bazhenov et al., 2016). The most complete lava sections of the Siberian Traps LIP from the Norilsk and Kotuy regions studied by (Heunemann et al., 2004; Pavlov et al., 2011a) demonstrate the less tight clustering too ($K = 39.0$ and $K = 56.5$, respectively). Thus, even for the Nizhnyaya Tunguska river intrusions the secular variations of the geomagnetic field can be not completely averaged pointing out to the quite intense magmatic activity, which lead to the formation of these intrusive complexes.

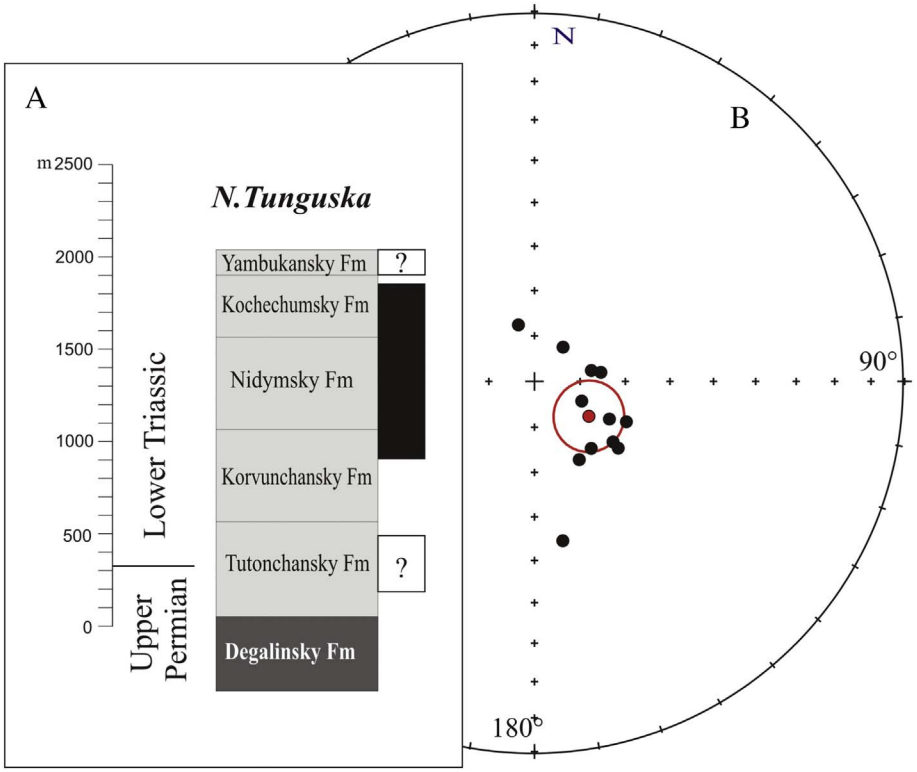

Fig. 7. Results of the paleomagnetic investigation of the volcanic section in the central part of the Tunguska syncline.
A – magnetic stratigraphy of the volcanic sequence. The normal polarity interval is shown as black rectangle, the suggested reversed intervals after (Sidoras, 1984) as white. The Permian-Triassic boundary is set according to (Domyshev, 1974).
B – site-mean directions (geographic coordinate system). Black circles are the sites with normal polarity, the red circle with the confidence interval is the mean for 12 sites. (For interpretation of the references to color in this figure legend, the reader is referred to the web version of this article.)

6.4. The volcanic section of the central part of the Tunguska syncline

The essential part of the volcanic pile in the Nizhnyaya Tunguska river valley (from the upper part of the Korvunchansky formation up to the Kochechumsky formation inclusively) was erupted during the single interval of normal polarity (Fig. 7A). It is consistent with the magnetostratigraphic scheme of the Tunguska syncline compiled by (Sidoras, 1984). It should be noted that at this moment we can neither confirm nor disprove the presence of reversed intervals in the youngest lavas of the Yambukansky formation and the oldest volcaniclastic deposits of the Tutonchansky formation suggested by (Sidoras, 1984). The site-mean paleomagnetic directions are shown on Fig. 7B. The shape of distribution appears to be elongate; however, the number of sites is insufficient for the reasonable discussion.

The $^{40}Ar/^{39}Ar$ data yielded from the Nidymsky formation basalts (251.8 ± 1.5 Ma and 248.9 ± 1.2 Ma (Reichow et al., 2009)) belong to the very beginning of the Early Triassic or the very end of the Late Permian. The Permian-Triassic boundary in the study of Reichow et al. (2009) was dated on sanidine crystals from bed 28 of Meishan stratotype section as 249.25 ± 0.14 Ma. This age cannot be directly compared to U-Pb age of the Permian-Triassic boundary (251.902 ± 0.024 Ma) obtained by Burgess et al. (2014) due to the ^{40}K decay uncertainties and calibrations of the $^{40}Ar/^{39}Ar$ standards. It is generally agreed that $^{40}Ar/^{39}Ar$ ages are about 1% systematically younger due to these problems (e.g. Renne et al., 2010, 2011; Ivanov et al., 2013). As mentioned above, three U-Pb age determinations for sills in the Nizhnyaya Tunguska river valley yielded tight clustering of ages (251.795 ± 0.070 Ma, 251.786 ± 0.054 Ma and 251.740 ± 0.180 Ma, Burgess and Bowring, 2015) at the very beginning of the Early Triassic. Based on the paleontological data the Korvunchansky formation is considered to be Early Triassic (e.g. Domyshev, 1974; Snigirevskaya and Mogucheva, 2010). Thus, at least one Late Permian $^{40}Ar/^{39}Ar$ age value is in disagreement with the paleontological data, whereas all other ages could be reconciled with paleontological data.

According to the most common correlation scheme for different regions of the Siberian Traps LIP on the basis of chemical compositions of lavas (e.g. Al'mukhamedov et al., 2004) the studied part of the Tunguska syncline section is coeval to the upper part of the Norilsk volcanic sequence (from the Morongovsky formation and higher), which has the normal polarity too (Heunemann et al., 2004; Pavlov et al., 2011a). However, similar chemistry does not necessary mean the same age (Ivanov et al., 2013). Considering all these facts we assume that the studied part of the Tunguska syncline volcanic section is Early Triassic, though other possibilities cannot be excluded at present.

In addition, we calculated the VGP for the studied volcanic sequence of the Tunguska syncline and compared it with the mean pole for the normal polarity interval from the Norilsk section (Pavlov et al., 2011a; Table 4). These poles appeared to be statistically indistinguishable: $\gamma/\gamma_{cr} = 11.1^{\circ}/11.2^{\circ}$. This fact does not contradict the correlation of the normal polarity intervals from the Tunguska syncline and Norilsk volcanic sequences.

Considering the duration of the normal polarity intervals in the Early Triassic according to the geomagnetic polarity timescale for the Triassic by (Hounslow and Muttoni, 2010), we can estimate the total duration of the volcanic activity in the central part of the Tunguska syncline. In this case the formation of the studied part of volcanic section along with sedimentary layers in the Nidymsky and Kochechumsky formation occurred during < 500–600 kyr.

6.5. The age of intrusions and their correlation with volcanic sections

Recently the development of geochronological methods has lead to the significant amount of high-precise U-Pb and $^{40}Ar/^{39}Ar$ data from the Siberian Traps (Kamo et al., 2003; Reichow et al., 2009; Ivanov et al., 2013; Burgess and Bowring, 2015). In spite of that, the above-mentioned ages from the Nizhnyaya Tunguska river sills are the only U-Pb data for the Tunguska syncline intrusions (Burgess and Bowring, 2015) and $^{40}Ar/^{39}Ar$ ages for one lava formation (Reichow et al., 2009). In Fig. 8 we show U-Pb and $^{40}Ar/^{39}Ar$ ages obtained by different authors from the intrusions of the Tunguska syncline and Angara-Taseeva depression, as well as from the Norilsk region. As seen in Fig. 8, U-Pb

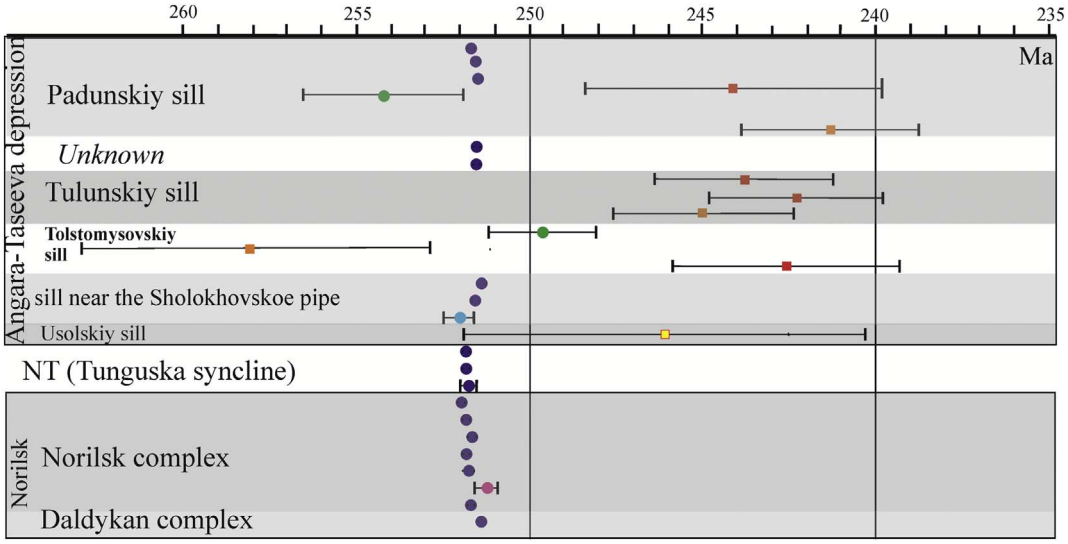

Fig. 8. U-Pb and $^{40}Ar/^{39}Ar$ ages of the intrusive Siberian Traps. U-Pb data (zircon) are shown as circles, $^{40}Ar/^{39}Ar$ (feldspar) – as squares. The colors mark the different sources: dark blue – (Burgess and Bowring, 2015); orange – (Ivanov et al., 2013); green – (Paton et al., 2010); red – (Ivanov et al., 2009); light blue – (Svensen et al., 2009); yellow – (Ivanov et al., 2005); pink – (Kamo et al., 1996). NT – the Nizhnyaya Tunguska river valley. Unknown – the geological affiliation of the dated intrusions is uncertain. For the majority of the ages from (Burgess and Bowring, 2015) the confidence intervals are not shown, because they are smaller than the symbol size. All $^{40}Ar/^{39}Ar$ data are recalculated by adding 0.9% to the age for the direct correlation with the U-Pb ages. (For interpretation of the references to color in this figure legend, the reader is referred to the web version of this article.)

ages of the Nizhnyaya Tunguska river intrusions are very close to U-Pb data from the other regions of the Siberian Traps LIP.

The small age variation for the distant from each other intrusions of the Nizhnyaya Tunguska river (about 0.1–0.2 Myr) indicates that the intense magmatic activity simultaneously took place in the vast area in the Siberian platform in the beginning of the Early Triassic (the distance of sampling exceeds 1000 km). However, the available data is not enough to exclude the possibility of wide-scale magmatic events of the significantly different age (for instance, the younger differentiated intrusions emplacement).

The majority of studied intrusions from the Nizhnyaya Tunguska river carries the normal polarity, as well as the explored interval of the Tunguska syncline volcanic section (from the uppermost Korvunchansky formation up to the Kochechumsky formation). The mean poles calculated for the volcanic section and normally magnetized intrusions (Table 4) are statistically indistinguishable: γ/γ_{cr} = 9.6°/10.6°. Thus, nothing contradicts the most apparent version that these normally magnetized intrusions and volcanic units were formed during the same interval of normal polarity in the Early Triassic.

The emplacement of the reversely magnetized bodies obviously either preceded or followed the eruption of the studied normally magnetized volcanic section. At this moment we can confidently claim that the intrusions of this group localized in the Nidymsky and upper Korvunchansky formations are younger that the main phase of volcanic activity in the Tunguska syncline and, possibly, in the whole Siberian platform.

The Angara-Taseeva depression sills represent the area with higher amount of both U-Pb and $^{40}Ar/^{39}Ar$ published ages (Fig. 8). The detailed review of the geochronological data was given by Ivanov et al. (2013). The above-mentioned $^{40}Ar/^{39}Ar$ ages from the sills of the Chuna river (Ivanov et al., 2009) are obtained from the objects belonging to the areas of the Padunskiy (241.9 ± 4.3 Ma) and Tulunskiy sills (241.6 ± 2.6 Ma).

Both Middle Triassic (about 240 Ma) $^{40}Ar/^{39}Ar$ ages (Ivanov et al., 2009, 2013) and significantly older U-Pb data (Burgess and Bowring, 2015; Paton et al., 2010) were obtained for the Padunskiy sill. The only one Late Permian $^{40}Ar/^{39}Ar$ age was also obtained for the Padunskiy sill (Ivanov et al., 2009). Though, the $^{40}Ar/^{39}Ar$ and U-Pb ages were not obtained on the same sites, the generally younger $^{40}Ar/^{39}Ar$ ages could be due to partial resetting of the K-Ar isotope systems in the sills. This is actually, quite common situation for other LIPs too. For example, $^{40}Ar/^{39}Ar$ ages for the Karoo-Ferrar province show large scatter in the range of > 10 Myr, whereas all single crystal U-Pb ages are clustering within < 1 Myr (e.g. Ivanov et al., 2017).

Considering this fact we prefer to use the data obtained by U-Pb method on single zircon grains in the same lab (Burgess and Bowring, 2015) for the direct correlation between the Angara-Taseeva depression and Tunguska syncline. The ages yielded by (Burgess and Bowring, 2015) for the dolerites of Padunskiy sill are 251.681 ± 0.063 Ma, 251.539 ± 0.056 Ma and 251.460 ± 0.051 Ma.

We compared U-Pb ages for the Padunskiy sill with the data obtained from other Siberian Trap LIP by the same authors (Burgess and Bowring, 2015). As shown in Fig. 8, the Padunskiy sill ages are regularly 0.1–0.3 Myr younger than those for the Nizhnyaya Tunguska river (though the errors for the youngest data from the Nizhnyaya Tunguska river and the oldest data from the Padunskiy sill overlap), but older than Daldykan complex from the Norilsk region (251.376 ± 0.050 Ma – see Fig. 8). The Daldykan intrusions, in turn, cut all the lava section of the Norilsk region (e.g. Ryabov et al., 2014) and have the reversed polarity (Lind et al., 1994). Thus, the Padunskiy sill emplacement probably took place just after the eruption the volcanic sequences of Norilsk region and the Tunguska syncline, those have the normal polarity and, consequently, right after the termination of the main volcanic phase of the Siberian LIP (Fig. 9).

As for the Tulunskiy sill, there are only $^{40}Ar/^{39}Ar$ ages, indicating the Middle Triassic time of its emplacement (Ivanov et al., 2009, 2013). Nevertheless, since all U-Pb data from Angara-Taseeva intrusions are significantly older (about 254–251 Ma - Svensen et al., 2009; Paton et al., 2010; Burgess and Bowring, 2015), we need the additional confirmation to establish the Middle Triassic age of the Tulunskiy sill decisively. The difference of the mean pole for the Tulunskiy sill from the NMK paleomagnetic pole cannot be the strong evidence for it because of insufficient averaging of the geomagnetic field variations (see Section 6.3).

6.6. Some features of the intrusive magmatic activity of the Siberian LIP

Based on the results of the detailed paleomagnetic investigation, we assume that the short bursts of magmatic activity simultaneously occurring in the vast area (~200–250 km in diameter) is the typical

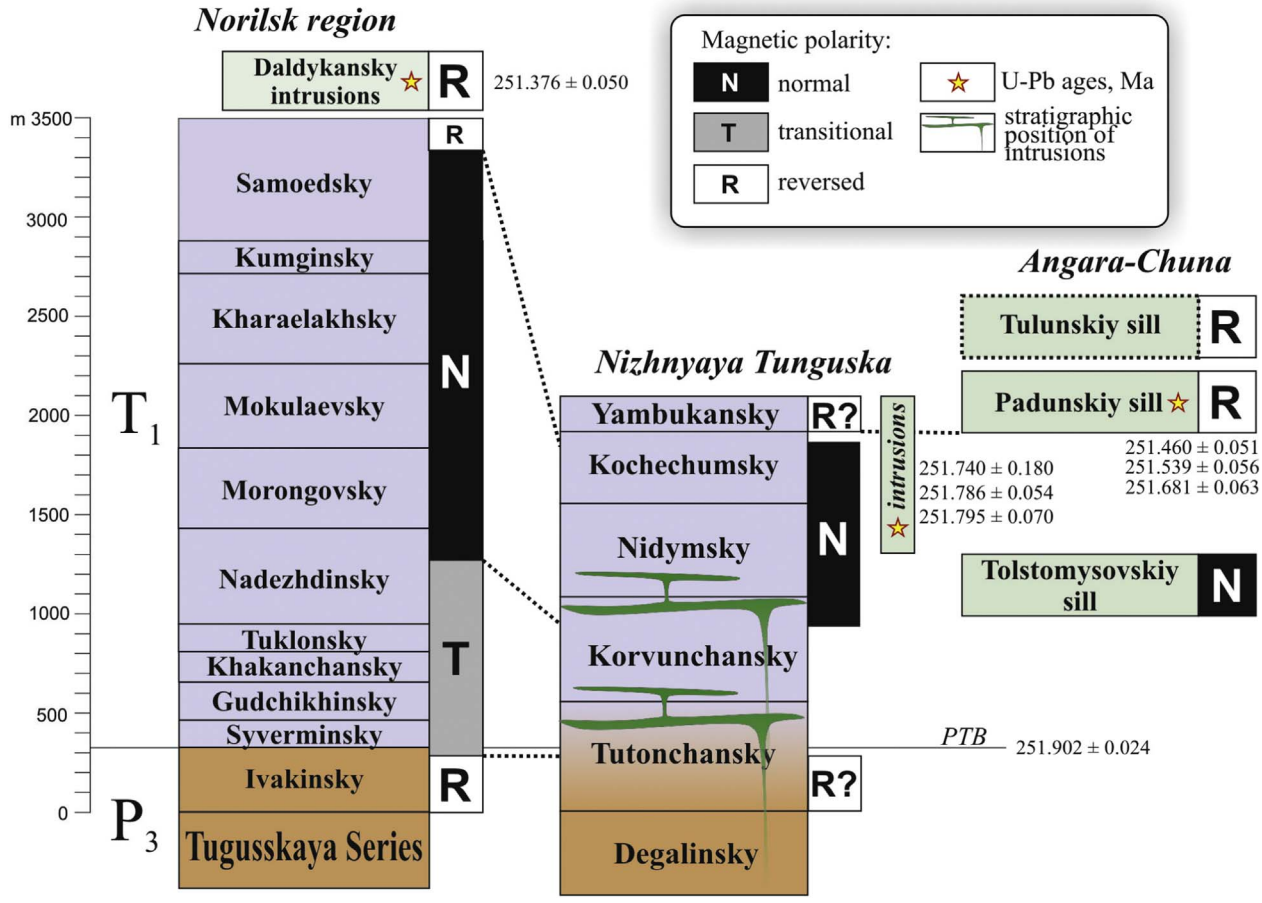

Fig. 9. The correlation of the studied intrusive complexes with volcanic sections of the Siberian Traps. The stratigraphic sequence and thickness is shown after (Fedorenko et al., 1996) for Norilsk region, after (Daragan-Sushchov, 1984; Domyshev, 1974) for the Nizhnyaya Tunguska river. The magnetic polarity is shown right of the columns after (Lind et al., 1994; Heunemann et al., 2004; Pavlov et al., 2015) for Norilsk region. U-Pb ages of intrusions are given after (Burgess and Bowring, 2015); the Permian-Triassic boundary age - after (Burgess et al., 2014). The position of the Tulunskiy sill is suppositional; the position of the Tolstomysovskiy sill is shown after (Latyshev et al., 2013).

feature of the magmatism in the Angara-Taseeva depression. The reversely magnetized Padunskiy and Tulunskiy sills as well as the normally magnetized Tolstomysovskiy sill (Latyshev et al., 2013) are the products of these intense magmatic events.

In the recent work (Konstantinov et al., 2014) the available paleomagnetic data from the Siberian Traps LIP intrusions are reviewed, and the objects with tightly grouped series of paleomagnetic directions ($K > 100$) are revealed. Similar directional groups are interpreted as the results of very rapid (a few thousand years) emplacement of the intrusive complexes. The most of tightly-clustered objects in this compilation are situated at the eastern periphery of the Tunguska syncline (four data sets from (Pavlov et al., 2007; Konstantinov et al., 2007; Konstantinov et al., 2014)). Moreover, we do not know the examples of representative data sets with more dispersed distribution of the paleomagnetic directions from the intrusions of the Tunguska syncline periphery. Hence, we conclude that the "pulsating" style of the intrusive magmatic activity expressed in the discrete voluminous magmatic events is common feature of the periphery (the southern and eastern margins) of the Tunguska syncline.

As was shown above, the studied intrusive complexes of the Nizhnyaya Tunguska river were formed longer than the discrete magmatic events in the Angara-Taseeva depression. At this moment we cannot distinguish any significant peaks of the magmatic activity. Nevertheless, some evidence like the proximity of U-Pb ages from the objects distant from each other, slightly lower amplitude of the geomagnetic field variations than expected (see Section 6.3) point out to the rather high intensity of the magmatism.

Considering the spatial distribution of the magmatic events, it should be noted that the areas of the exposure for the Padunskiy and Tulunskiy sill do not overlap (Fig. 1B), as well as for the Tolstomysovskiy sill (Latyshev et al., 2013). On the contrary, among the studied intrusions of the Nizhnyaya Tunguska river sites with normal and reversed polarity irregularly alternate along the river (Fig. 1C). Therefore, we can identify another difference in the character of magmatic activity in the central and marginal zones of the Tunguska syncline. Within the Angara-Taseeva depression, the most part of the territory underwent to the voluminous and intense but one-act magmatic manifestations. In the central part of the Tunguska syncline intrusive events were rather local and evenly distributed over the time, and, probably, were related with multiple volcanic episodes.

To reveal the complete pattern of the intrusive magmatic activity during the Siberian Traps emplacement, we should discuss the data from the Norilsk and Maymecha-Kotuy regions, where the thickest lava sections are reported (Fedorenko et al., 1996; Fedorenko and Czamanske, 1997). In the Norilsk region, from 7 to 10 intrusive complexes are distinguished (Malich et al., 1991; Radko, 2016), including the ore-bearing Norilsk- and Lower Talnakh-type intrusions. Unfortunately, the paleomagnetic data from the intrusions of Norilsk region are fragmentary and obtained without using the full demagnetization (Lind et al., 1994). The detailed paleomagnetic investigation of the intrusions from Norilsk region is the goal of the further research.

Paleomagnetic data from the dike complexes of the northern slope of the Anabar shield and Maymecha-Kotuy region were reported by Veselovskiy et al. (2012). Several reported data sets demonstrated more dispersed paleomagnetic directions ($K = 20–65$) compared with intrusions studied in this work, wherein the values of VGP scatter are

confident with TK03 model (Tauxe and Kent, 2004). We suggest that such values of these parameters correspond to less intensive style of intrusive activity. Taken together with the local distribution of dikes belonging to different geochemical types (Fedorenko et al., 2000), these features of magmatism could be explained by generally rift-related mode of the Permian-Triassic magmatic activity in Maymecha-Kotuy region and its eastward extension, unlike the “flood-basalt”, typical “traps” volcanism in the Tunguska syncline.

Finally, we note that the intrusive complexes younger than the main part of the volcanic sequence are widely distributed both in the Angara-Taseeva depression and the Tunguska syncline (e.g. the large Padunskiy sill and associated intrusions, as well as reversely magnetized sills and dikes in the Tunguska syncline). This fact indirectly confirms that the initial volume of the Permian-Triassic Siberian Traps LIP significantly exceeded that preserved today.

7. Conclusions

1. The products of brief intense magmatic events are widely distributed within the Angara-Taseeva depression (the Padunskiy, Tulunskiy and Tolstomysovskiy sills). The pulsating style of magmatic activity with discrete and short, but voluminous magmatic events, is typical for the periphery of the Tunguska syncline.
2. In the central part of the Tunguska syncline (the Nizhnyaya Tunguska river valley) the emplacement of intrusions occurred during at least two intervals of the normal and reverse polarity of the geomagnetic field. Generally, the magmatic activity in the center of the syncline occurred more evenly than in the periphery, and the magmatic events were rather local.
3. The essential part of the volcanic sequence in the Tunguska syncline (from the uppermost Korvunchansky formation up to Kochechumsky formation) erupted during one interval of the normal polarity, most likely, in the Early Triassic. The duration of emplacement of this part of the section, probably, did not exceed 500–600 kyr.
4. The Padunskiy sill and related intrusions were formed just after the termination of the main phase of the Permian-Triassic volcanic activity on the Siberian platform. In total, the intrusions younger than the volcanic section are widely distributed within the Siberian Traps LIP. However, the total duration of the magmatism is not yet established. Especially, $^{40}Ar/^{39}Ar$ ages have to be confirmed or disproved by U-Pb dating.

Acknowledgements

This study was funded by Russian Foundation for Basic Research (projects Nos. 16-35-60114, 15-35-20599, 15-05-05130) and the Ministry of Education and Science RF (project No. 14.Z50.31.0017). The authors gratefully thank M.L. Bazhenov for the productive discussion of the work, V.E. Pavlov for the helpful comments to the paper, P.S. Ulyahina an E.M. Mirsayanova for the participation in the field and laboratory investigation.

References

Al'mukhamedov, A.I., Medvedev, A.Ya., Zolotukhin, V.V., 2004. Chemical evolution of the Permian-Triassic basalts of the Siberian platform in space and time. Petrology 12, 297–311.

Bazhenov, M.L., Van der Voo, R., Menzo, Z., Domingez, A.R., Meert, J.G., Levashova, N.M., 2016. Paleomagnetism and dating of a thick lava pile in the Permian Bakaly formation of Eastern Kazakhstan: regularities and singularities of the paleomagnetic record in thick lava series. Phys. Earth Planet. Inter. 253, 5–20. https://doi.org/10.1016/j.pepi.2016.02.001.

Beck, M.E., 1999. On the shape of paleomagnetic data sets. J. Geophys. Res. 104 (B11), 25427–25441.

Blackburn, T.J., Olsen, P.E., Bowring, S.A., McLean, N.M., Kent, D.V., Puffer, J., McHone, G., Rasbury, E.T., Et-Touhami, M., 2013. Zircon U-Pb geochronology links the end-Triassic extinction with the Central Atlantic Magmatic Province. Science 340, 941–945.

Burgess, S.D., Bowring, S.A., 2015. High-precision geochronology confirms voluminous magmatism before, during, and after Earth's most severe extinction. Sci. Adv. 1 (7). http://dx.doi.org/10.1126/sciadv.1500470.

Burgess, S.D., Bowring, S.A., Shen, S.-Z., 2014. High-precision timeline for Earth's most severe extinction. Proc. Natl. Acad. Sci. U. S. A. 111, 3316–3321.

Burgess, S.D., Bowring, S.A., Fleming, T.H., Elliot, D.H., 2015. High-precision geochronology links the Ferrar large igneous province with early-Jurassic anoxia and biotic crisis. Earth Planet. Sci. Lett. 415, 90–99. http://dx.doi.org/10.1016/j.epsl.2015.01.037.

Burgess, S.D., Muirhead, J.D., Bowring, S.A., 2017. Initial pulse of Siberian Traps sills as the trigger of the end-Permian mass extinction. Nat. Commun. 8 (164), 1–6. http://dx.doi.org/10.1038/s41467-017-00083-9.

Buslov, M.M., Safonova, I.Yu., Fedoseev, G.S., Reichow, M.K., Davies, K., Babin, G.A., 2010. Permo-Triassic plume magmatism of the Kuznetsk Basin, Central Asia: geology, geochronology, and geochemistry. Russ. Geol. Geophys. 51 (9), 1021–1036.

Chadima, M., Hrouda, F., 2006. Remasoft 3.0 a user-friendly paleomagnetic data browser and analyzer. Travaux Géophysiques XXVII, 20–21.

Chenet, A.L., Fluteau, F., Courtillot, V., Gerard, M., Subbarao, K.V., 2008. Determination of rapid Deccan eruptions across the Cretaceous-Tertiary boundary using paleomagnetic secular variation: results from a 1200-m-thick section in the Mahabaleshwar escarpment. J. Geophys. Res. 113 (B04101). http://dx.doi.org/10.1029/2006JB004635.

Chenet, A.L., Courtillot, V., Fluteau, F., Gerard, M., Quidelleur, X., Khadri, S.F.R., Subbarao, K.V., Thordarson, T., 2009. Determination of rapid Deccan eruptions across the Cretaceous-Tertiary boundary using paleomagnetic secular variation: 2. Constraints from analysis of eight new sections and synthesis for a 3500-m-thick composite section. J. Geophys. Res. 114 (B06103). http://dx.doi.org/10.1029/2008JB005644.

Courtillot, V.E., Renne, P.R., 2003. On the ages of flood basalt events. C. R. Geosci. 335, 113–140.

Crouzet, C., Rochette, P., Ménard, G., 2001. Experimental evaluation of thermal recording of successive polarities during uplift of metasediments. Geophys. J. Int. 145, 771–785.

Czamanske, G.K., Gurevich, A.B., Fedorenko, V., Simonov, O., 1998. Demise of the Siberian plume: paleogeographic and paleotectonic reconstruction from the pre-volcanic and volcanic records, North-Central Siberia. Int. Geol. Rev. 40, 95–115.

Daragan-Sushchov, Yu.I., 1984. The formation of volcanic sequence of the Tunguska syncline. PhD Thesis. Leningrad. (in Russian).

Day, R., Fuller, M., Schmidt, V.A., 1977. Hysteresis properties of titanomagnetites: grain-size and compositional dependence. Phys. Earth Planet. Inter. 13, 260–267.

Domyshev, V.G., 1974. Piroclastic Deposits, Trap Magmatism and Tectonics of the South-East Tunguska Syncline. (Nauka. 118 p. in Russian).

Elkins-Tanton, L.T., 2005. Continental magmatism caused by lithospheric delamination. In: Foulger, G.R. (Ed.), Plates, Plumes and Paradigms. Princeton: Geological Society of America Special Paper 388, pp. 449–462.

Enkin, R.J., 1994. A computer program package for analysis and presentation of paleomagnetic data. In: Pacific Geoscience Centre, Geological Survey of Canada, pp. 16.

Fedorenko, V., Czamanske, G., 1997. Results of New Field and Geochemical Studies of the Volcanic and Intrusive Rocks of the Maymecha-Kotuy Area, Siberian Flood-Basalt Province, Russia. Int. Geol. Rev. 39, 479–531.

Fedorenko, V.A., Lightfoot, P.C., Naldrett, A.J., et al., 1996. Petrogenesis of the flood-basalt sequence at Noril'sk, North-Central Siberia. Int. Geol. Rev. 38, 99–135.

Fedorenko, V., Czamanske, G., Zen'ko, T., Budahn, J., Siems, D., 2000. Field and geochemical studies of the melilite-bearing Arydzhangsky Suite, and an overall perspective on the Siberian alkaline-ultramafic flood-volcanic rocks. Int. Geol. Rev. 42 (9), 769–804.

Feoktistov, G.D., 1978. Petrology and Conditions of Trap Sills Formation. Nauka, Novosibirsk. (166 pp. in Russian).

Fetisova, A.M., Veselovskiy, R.V., Latyshev, A.V., Rad'ko, V.A., Pavlov, V.E., 2014. Magnetic stratigraphy of the Permian–Triassic Traps in the Kotui River Valley (Siberian Platform): New Paleomagnetic Data. Stratigr. Geol. Correl. 22 (4), 377–390.

Fisher, R., 1953. Dispersion on a sphere. Proc. R. Soc. Lond. A Math. Phys. Sci. 217 (1130), 295–305.

Gurevitch, E.L., Westphal, M., Daragan-Suchov, J., Feinberg, H., Pozzi, J.P., Khramov, A.N., 1995. Paleomagnetism and magnetostratigraphy of the traps from Western Taimyr (northern Siberia) and the Permo-Triassic crisis. Earth Planet. Sci. Lett. 136 (3–4), 461–473.

Gurevitch, E.L., Heunemann, C., Rad'ko, V., Westphal, M., Bachtadse, V., Pozzi, J.P., Feinberg, H., 2004. Palaeomagnetism and magnetostratigraphy of the Permian–Triassic northwest central Siberian Trap Basalts. Tectonophysics 379, 211–226.

Heunemann, C., Krasa, D., Soffel, H., Gurevitch, E., Bachtadse, V., 2004. Directions and intensities of the Earth's magnetic field during a reversal: results from the Permo-Triassic Siberian trap basalts, Russia. Earth Planet. Sci. Lett. 218, 197–213.

Hounslow, M., Muttoni, G., 2010. The geomagnetic polarity timescale for the Triassic: linkage to stage boundary definitions. In: The Triassic Timescale. Geological Society of London, London, pp. 61–102.

Irving, E., 1964. Paleomagnetism and Its Application to Geological and Geophysical Problems. Wiley, New York (399 p).

Ivanov, A.V., 2007. Evaluation of different models for the origin of the Siberian Traps. In: Foulger, G.R., Jurdy, D.M. (Eds.), Plates, Plumes and Planetary Processes. Geological Society of America Special Paper 430, pp. 669–691.

Ivanov, A.V., Rasskazov, S.V., Feoktistov, G.D., He, H., Boven, A., 2005. $^{40}Ar/^{39}Ar$ dating of Usol'skii sill in the southeastern Siberian Traps Large Igneous Province: evidence for long-lived magmatism. Terra Nova 17, 203–208.

Ivanov, A.V., He, H., Yang, L., Nikolaeva, I.V., Palesskii, S.V., 2009. $^{40}Ar/^{39}Ar$ dating of

intrusive magmatism in the Angara-Taseevskaya syncline and its implication for duration of magmatism of the Siberian Traps. J. Asian Earth Sci. 35, 1–12.
Ivanov, A.V., He, H., Yan, L., Ryabov, V.V., Shevko, A.Y., Palesskii, S.V., Nikolaeva, I.V., 2013. Siberian Traps large igneous province: evidence for two flood basalt pulses around the Permo–Triassic boundary and in the Middle Triassic, and contemporaneous granitic magmatism. Earth-Sci. Rev. 122, 58–76. https://doi.org/10.1016/j.earscirev.2013.04.001.
Ivanov, A.V., Meffre, S., Thompson, J., Corfu, F., Kamenetsky, V.S., Kamenetsky, M.B., Demonterova, E.I., 2017. Timing and genesis of the Karoo-Ferrar large igneous province: New high precision U-Pb data for Tasmania confirm short duration of the major magmatic pulse. Chem. Geol. 435, 32–43. https://doi.org/10.1016/j.chemgeo.2016.10.008.
Jourdan, F., Feraud, G., Bertrand, H., Watkeys, M.K., Renne, P.R., 2007. Distinct brief major events in the Karoo Large Igneous Province clarified by new $^{40}Ar/^{39}Ar$ ages on the Lesoto Basalts. Lithos 98, 195–209.
Kamo, S.L., Czamanske, G.K., Krogh, T.E., 1996. A minimum U-Pb age for Siberian flood-basalt volcanism. Geochim. Cosmochim. Acta 60 (18), 3505–3511.
Kamo, S.L., Czamanske, G.K., Amelin, Yu., Fedorenko, V.A., Davis, D.W., Trofimov, V.R., 2003. Rapid eruption of Siberian flood-volcanic rocks and evidence for coincidence with the Permian-Triassic boundary and mass extinction at 251 Ma. Earth Planet. Sci. Lett. 214, 75–91.
Kirschvink, J.L., 1980. The least-square line and plane and the analysis of paleomagnetic data. Geophys. J. R. Astron. Soc. 62, 699–718.
Konstantinov, K.M., Mishenin, S.G., Kuzmenok, A.N., Tomshin, M.D., Gladkov, A.S., Vasilyeva, A.E., 2007. Petromagnetic heterogeneities of the Permian–Triassic traps in the Daldyn-Alakit area and their significance for diamond pipe prospecting. In: Proceedings of Symposium "Paleomagnetism and Petromagnetism: Theory, Practice, Experiment", Borok, GEOS, pp. 63–69 (in Russian).
Konstantinov, K.M., Bazhenov, M.L., Fetisova, A.M., Khutorskoy, M.D., 2014. Paleomagnetism of trap intrusions, East Siberia: implications to flood basalt emplacement and the Permo–Triassic crisis of biosphere. Earth Planet. Sci. Lett. 394, 242–253.
Krivolutskaya, N.A., 2016. Siberian Traps and Pt-Cu-Ni deposits in the Noril'sk area. Springer International Publishing, pp. 1–364.
Latyshev, A.V., Veselovsky, R.V., Ivanov, A.V., Fetisova, A.V., Pavlov, V.E., 2013. Short intense bursts in magmatic activity in the south of Siberian Platform (Angara-Taseeva Depression): the paleomagnetic evidence. Izv. Phys. Solid Earth 49 (6), 823–835.
Lind, E., Kropotov, S., Czamanske, G., Gromme, S., Fedorenko, V., 1994. Paleomagnetism of the Siberian flood basalts of the Norilsk area: a constraint on eruption duration. Int. Geol. Rev. 36 (12), 1139–1150.
Malich, N.S., Mkrtychyan, A.K., Strunin, B.M., 1991. The Geological map of the Norilsk ore region of 1: 200 000 scale. Krasnoyarskgeologiya. .
Masaitis, V.L., 1983. Permian and Triassic volcanism of Siberia. Zap. Vses. Mineral. O-va. 4, 412–425 (In Russian).
McElhinny, M.W., McFadden, P.L., 1997. Palaeosecular variation over the past 5 Myr based on a new generalized database. Geophys. J. Int. 131 (2), 240–252.
McFadden, P.L., McElhinny, M.W., 1990. Classification of the reversal test in palaeomagnetism. Geophys. J. Int. 103, 725–729.
Moulin, M., Fluteau, F., Courtillot, V., Marsch, J., Delpech, G., Quidelleur, X., Gerard, M., Jay, A.E., 2011. An attempt to constrain the age, duration, and eruptive history of the Karoo flood basalt: Naude's Nek section (South Africa). J. Geophys. Res. 116 (B07403). http://dx.doi.org/10.1029/2011JB008210.
Naldrett, A.J., Fedorenko, V.A., Asif, M., Lin, M., Kunilov, V.E., Stekhin, A.I., Lightfoot, P.C., Gorbachev, N.S., 1996. Controls of the compositions of Ni-Cu sulfide deposits as illustrated by those at Noril'sk, Siberia. Econ. Geol. 87, 975–1004.
Pan, Y., Qin, H., He, H., Ivanov, A., Cai, S., Liu, C., Paterson, G.A., Zhu, R., 2013. Dipole low at the Permo-Triassic boundary? New paleomagnetic data from the central Siberian Traps. In: American Geophysical Union, Fall Meeting, (abstract #GP53D-08).
Paton, M.T., Ivanov, A.B., Fiorentini, M.L., McNaughton, N.J., Mudrovska, I., Demonterova, E.I., 2010. Late Permian and Early Triassic magmatic pulses in the Angara–Taseeva syncline South Siberian Traps and their possible influence on the environment. Russ. Geol. Geophys. 51, 1012–1020.
Pavlov, V.E., Courtillot, V., Bazhenov, M.L., Veselovsky, R.V., 2007. Paleomagnetism of the Siberian traps: new data and a new overall 250 Ma pole for Siberia. Tectonophysics 443, 72–92.
Pavlov, V.E., Fluteau, F., Veselovskiy, R.V., Fetisova, A.M., Latyshev, A.V., 2011a. Secular geomagnetic variations and volcanic pulses in the Permian–Triassic traps of the Norilsk and Maimecha–Kotui provinces. Izv. Phys. Solid Earth 47 (5), 402–417.
Pavlov, V.E., Veselovskiy, R.V., Khokhlov, A., Latyshev, A.V., Fluteau, F., 2011b. Refined Permo-Triassic Paleomagnetic Pole for the Siberian Platform and Geomagnetic Secular Variations at the Paleozoic-Mesozoic Boundary as Recorded in Volcanic Traps Key Sections of Northern Siberia. Am. Geophys. Union, Fall Meeting (Abstract GP11A-0999).
Pavlov, V.E., Veselovskiy, R.V., Shatsillo, A.V., Gallet, Y., 2012. Magnetostratigraphy of the Ordovician Angara/Rozhkova river section: further evidence for the Moyero reversed superchron. Izv. Phys. Solid Earth 48 (4), 297–305.
Pavlov, V., Fluteau, F., Veselovskiy, R., Fetisova, A., Latyshev, A., Elkins-Tanton, L.T., Sobolev, A.V., Krivolutskaya, N.A., 2015. In: Schmidt, A., Fristad, K.E., Elkins-Tanton, L. (Eds.), Volcanic Pulses in the Siberian Traps as Inferred From Permo-Triassic Geomagnetic Secular Variations. Chapter 5 in "Volcanism and Global Environmental Change". Cambridge University Press, pp. 63–78.
Radko, V.A., 2016. The Facies of Intrusive and Effusive Magmatism in the Norilsk Region. — St. Petersburg: Cartographic Factory of VSEGEI. (226 p).
Reichow, M.K., Saunders, A.D., White, R.V., Al'mukhamedov, A.I., Medvedev, A.Ya, 2005. Geochemistry and petrogenesis ob basalts from the West Siberian Basin: an extension of the Permo-Triassic Traps, Russia. Lithos 79, 425–452. http://dx.doi.org/10.1016/j.lithos.2004.09.011.
Reichow, M.K., Pringle, M.S., Al'Mukhamedov, A.I., Allen, M.B., Andreichev, V.L., Buslov, M.M., Davies, C., Fedoseev, G.S., Fitton, J.G., Inger, S., Medvedev, A.Ya., Mitchell, C., Puchkov, V.N., Safonova, I.Yu., Scott, R.A., Saunders, A.D., 2009. The timing and extent of the eruption of the Siberian traps large Igneous Province: implications for the end-Permian environmental crisis. Earth Planet. Sci. Lett. 277 (1–2), 9–20.
Renne, P.R., Mundil, R., Balco, G., Min, K., Ludwig, K.R., 2010. Joint determination of ^{40}K decay constants and $^{40}Ar^*/^{40}K$ for the Fish Canyon sanidine standard, and improved accuracy for $^{40}Ar/^{39}Ar$ geochronology. Geochim. Cosmochim. Acta 74, 5349–5367. http://dx.doi.org/10.1016/j.gca.2010.06.017.
Renne, P.R., Balco, G., Ludwig, K.R., Mundil, R., Min, K., 2011. Response to the comment by W.H. Schwarz et al. on "Joint determination of ^{40}K decay constant and $^{40}Ar^*/^{40}K$ for the Fish Canyon sanidine standard, and improved accuracy for $^{40}Ar/^{39}Ar$ geochronology" by P.R. Renne et al. (2010). Geochim. Cosmochim. Acta 75, 5097–5100. http://dx.doi.org/10.1016/j.gca.2011.06.021.
Renne, P.R., Sprain, C.J., Richards, M.A., Self, S., Vanderkluysen, L., Pande, K., 2015 Oct 2. State shift in Deccan volcanism at the cretaceous-Paleogene boundary, possibly induced by impact. Science 350 (6256), 76–78. http://dx.doi.org/10.1126/science.aac7549.
Rochette, P., Ménard, G., Dunn, R., 1992. Thermochronometry and cooling rates deduced from single sample records of successive magnetic polarities during uplift of metamorphic rocks in the Alps (France). Geophys. J. Int. 108, 491–501.
Ryabov, V.V., Shevko, A.Ya., Gora, M.P., 2014. Trap Magmatism and Ore Formation in the Siberian Noril'sk Region. Volume 1. Trap Petrology. Modern Approaches in Solid Earth Sciences. Volume 3.
Saunders, A., Reichow, M., 2009. The Siberian Traps and the End-Permian mass extinction: a critical review. Chin. Sci. Bull. 54 (1), 20–37.
Schoene, B., Samperton, K.M., Eddy, M.P., Keller, G., Adatte, T., Bowring, S.A., Khadri, S.F.R., Gertsch, B., 2015. U-Pb geochronology of the Deccan Traps and relation to the end-Cretaceous mass extinction. Science 347, 182–184.
Sell, B., Ovtcharova, M., Guex, J., Bartolini, A., Jourdan, F., Spangenberg, J.E., Vicente, J.-C., Schaltegger, U., 2014. Evaluating the temporal link between the Karoo LIP and climatic-biologic events of the Toarcian Stage with high-precision U-Pb geochronology. Earth Planet. Sci. Lett. 408, 48–56. http://dx.doi.org/10.1016./j.epsl.2014.10.008.
Shcherbakov, V.P., Latyshev, A.V., Veselovskiy, R.V., Tselmovich, V.A., 2017. Origin of false remanence at conventional stepwise thermal demagnetization. Russ. Geol. Geophys. 58, 1118–1128.
Sidoras, S.D., 1984. Magnetism of the Volcanic Formations of the Tunguska Syncline and its Importance for the Geological Research. PhD Thesis. Leningrad (206 p. in Russian).
Snigirevskaya, N.S., Mogucheva, N.K., 2010. A Find of the Fossilized Root Chromorphyza Gen. N. (Pinopsida Incertae Sedis) in Triassic Peosits of the Putorana Plateau (the Tunguska syncline) and its Scientific Importance. *Paleontology and Stratigraphy News*. 14. pp. 37–50 (in Russian).
Sobolev, S.V., Sobolev, A.V., Kuzmin, D.V., Krivolutskaya, N.A., Petrunin, A.G., Arndt, N.T., Rad'ko, V.A., Vasil'yev, Y.R., 2011. Linking mantle plumes, large igneous provinces, and environmental catastrophes. Nature. http://dx.doi.org/10.1038/nature10385.
Svensen, H., Planke, S., Polozov, A.G., Schmidbauer, N., Corfu, F., Podladchikov, Y.Y., Jamtveit, B., 2009. Siberian gas venting and the end-Permian environmental crisis. Earth Planet. Sci. Lett. 277, 490–500.
Svensen, H., Corfu, F., Polteau, S., Hammer, Ø., Planke, S., 2012. Rapid magma emplacement in the Karoo Large Igneous Province. Earth Planet. Sci. Lett. 325–326, 1–9.
Tauxe, L., Kent, D.V., 2004. A simplified statistical model for the geomagnetic field and the detection of shallow bias in paleomagnetic inclinations: Was the ancient magnetic field dipolar? In: Channell, J.E.T. (Ed.), Timescales of the Paleomagnetic Field. Am. Geophys. Union 145.
Tauxe, L., Shaar, R., Jonestrask, L., Swanson-Hysell, N.L., Minnett, R., Koppers, A.A.P., Constable, C.G., Jarboe, N., Gaastra, K., Fairchild, L., 2016a. PmagPy: software package for paleomagnetic data analysis and a bridge to the magnetic information consortium (MagIC) database. Geochem. Geophys. Geosyst. 17, 2450–2463. http://dx.doi.org/10.1002/2016GC006307.
Tauxe, L., Banerjee, S.K., Butler, R.F., Van der Voo, R., 2016b. Essentials of Paleomagnetism, 4rd Web Edition. .
Veselovskiy, R.V., Konstantinov, K.M., Latyshev, A.V., Fetisova, A.M., 2012. Paleomagnetism of the trap intrusive bodies in Arctic Siberia: geological and methodical implications. Izv. Phys. Solid Earth 48 (9–10), 738–750.
Vyssotski, A.V., Vyssotski, V.N., Nezhdanov, A.A., 2006. Evolution of the West Siberian Basin. Mar. Pet. Geol. 23, 93–126.
Zolotukhin, V.V., Vilenskii, A.M., Dyuzhikov, O.A., 1986. Basalts of Siberian Platform. Nauka, Novosibirsk (in Russian).